Annu. Rev. Astron. Astrophys. 1999. 37:127–89

PROBING THE UNIVERSE WITH WEAK LENSING

Yannick Mellier[1,2]
[1]*Institut d'Astrophysique de Paris, 98 bis Boulevard Arago, 75014 Paris, France.*
[2]*Observatoire de Paris, DEMIRM, 61 avenue de l'Observatoire, 75014 Paris, France; E-mail: mellier@iap.fr*

Key Words cosmology, gravitational lensing, dark matter, clusters of galaxies, evolution of galaxies

■ **Abstract** Gravitational lenses can provide crucial information on the geometry of the Universe, on the cosmological scenario of formation of its structures as well as on the history of its components with look-back time. In this review, I focus on the most recent results obtained during the last five years from the analysis of the weak lensing regime. The potential of weak lensing as a probe of dark matter and the study of the coupling between light and mass on scales of clusters of galaxies, large-scale structures and galaxies is discussed first. Then I present the impact of weak lensing for the study of distant galaxies and of the population of lensed sources as a function of redshift. Finally, I discuss the potential of weak lensing to constrain the cosmological parameters, either from pure geometrical effects observed in peculiar lenses, or from the coupling of weak lensing with the CMB.

1. INTRODUCTION

Matter intervening along the light paths of photons causes a displacement and a distortion of ray bundles. The properties and the interpretation of this effect depend on the projected mass density integrated along the line of sight and on the cosmological angular distances to the observer, the lens and the source.

The sensitivity to mass density implies that gravitational lensing effects can probe the mass of deflectors, without regard to their dynamical stage and the nature of the deflecting matter. This is therefore a unique tool to probe the dark matter distribution in gravitational systems as well as to study the dynamical evolution of structures with redshift. The dependence on the various angular distances involved in the lens configuration means that the deviation angle depends on the cosmological parameters, H_o, Ω and λ, so that the analysis of gravitational lensing can potentially provide a diagnosis on cosmography. Of course, the sensitivity to cosmological parameters is not unique to gravitational lensing, and many other astrophysical phenomena depend on them. However, owing to magnification, image multiplicity and deflection angle produced by lensing, it is possible to use the lensing effect as a bonus when compared with other experiments: image

magnification permits observation of the high-redshift universe, study of the evolution of galaxies with look-back time and comparison with theoretical cosmological scenarios. Image multiplicity probes different light paths taken by photons emitted by one source. By computing time delays of the same transient event observed in each individual image, one can measure H_o. Finally, for high-redshift sources the deflecting angle depends on the geometry of the universe and provides a unique tool for measuring the cosmological parameters.

The interest in gravitational lensing for cosmology started very early, after Zwicky's discovery (Zwicky 1933) of the apparent contradiction between the visible mass of the Coma cluster and its virial mass, which could not be explained without recognizing that it is dominated by *unseen mass*. This surprising statement could not be confirmed without an independent mass estimator, which could probe the total mass directly, without using the light distribution or critical assumptions on the dynamical stage of the cluster components. Four years later, Zwicky (1937) envisioned that *extragalactic nebulae* could be efficient gravitational lenses and provide an invaluable tool for weighting the gravitational systems of the Universe.

The other works that raised interest in lensing for cosmology are more contemporary. Refsdal (1964) first emphasized that time delays in multiple images could be used to measure H_o, and the very first considerations of light propagation and deformation of ray bundles in inhomogeneous universes were discussed initially by Sachs (1961) and Zel'dovich (1964) and later by Gunn (1967). From an observational point of view, the discoveries of the first multiply imaged quasar (Walsh et al 1979) and the first distorted galaxies (Soucail et al 1987, Lynds & Petrosian 1986) were major steps that boosted theoretical and observational investigations of gravitational lenses.

Most of the cosmological interest in gravitational lenses has already been reviewed by Blandford & Narayan (1992), Schneider et al (1992) and Refsdal & Surdej (1994). Fort & Mellier (1994) presented the first review which focused particularly on the use of arc(let)s in cosmology, and the interest in the use of lensed galaxies to probe the deep universe has been recently reviewed by Ellis (1997). With the amazing observational and theoretical developments in the field, in particular in weak lensing, it seems timely to review all these results and to address the new and future issues in the area.

During the last five years, thanks to the seminal work on mass reconstruction from weak lensing analyses (Tyson et al 1990, Kaiser & Squires 1993), mass reconstruction algorithms have provided new and robust tools for studying the mass distribution of gravitational systems and have permitted the establishment of a link between theoretical investigations of weak lensing and the observations of weakly distorted galaxies. In particular, there have been impressive developments in cosmological diagnoses from the analysis of weak lensing induced by large-scale structures. Theoretical and numerical studies demonstrate that the statistical analysis of gravitational lensing will provide valuable insights on the mass distribution as well as on the cosmological parameters. With the coming

of new wide field surveys with subarcsecond seeing [such as Megacam at the Canada-France-Hawaii Telescope (CFHT) or the VLT-Survey-Telescope (VST) at Paranal] or very wide field shallow surveys [such as the VLA-Faint Images of the Radio Sky at Twenty-Centimeters (FIRST) survey or the Sloan Digital Sky Survey (SDSS)], weak-lensing analysis should probe the power spectrum of the projected mass density, from arcminutes up to degree scales. Visible weak lensing surveys should also be capable of providing a projected mass map of the universe, just as the Automated Plate Machine (APM) survey provides the visible light distribution (Maddox et al 1990). From the observational point of view, the outstanding images coming from Hubble Space Telescope (HST) had a considerable positive impact on our intuitions about the potential usefulness of gravitational distortion. The wonderful shear pattern around lensing cluster A2218 is visual proof that weak lensing works and that it directly reveals the mass distribution. One of the most spectacular uses of HST images for lensing was done by Kneib et al (1996), also in A2218. The superb HST images allowed them to demonstrate, from the morphology of only one arclet, and without the need of a spectroscopic redshift, that it must be a lensed image associated with the same source as the giant arc. The similarity of the morphologies of the giant arc and the counter-image is so impressive that it cannot be questioned that they are images of the same source. In parallel, the Keck telescope, which is currently detecting the most distant galaxies, reveals the obvious importance of *giant gravitational telescopes*. Finally, the impressive results obtained by the Submillimetre Common-User Bolometer Array (SCUBA) in the submillimeter wavebands have shown that the joint use of a submillimeter instrument with magnification of high-redshift galaxies is an ideal tool for studying the evolution and content of distant galaxies.

In the following I review most of these recent works and discuss their impact for cosmology. Although this review focuses on weak lensing, the distinction between arclets and the weak lensing regime is somewhat arbitrary, and both are relevant for our purpose. Furthermore, because some of the results cannot be discussed without referring to strong lensing, I often include new results from arcs and multiple image studies. Section 2 recalls the basic equations useful in gravitational lensing which help in the understanding of this review. The definitions for strong lensing cases are not presented again, and I will refer to the review by Fort & Mellier (1994) for all these aspects. In Section 3 I focus on the mass distribution in clusters of galaxies from arc(let)s or mass reconstruction from weak lensing inversion. I also address the issues concerning the measurement of weak shear because it appears to be a major challenge for observers. Section 4 presents weak lensing induced by large-scale structures, and Section 5 presents weak lensing induced by foreground galaxies on the background sources (the so-called galaxy-galaxy lensing analysis). I then move toward the high-redshift universe in Section 6. Sections 7 and 8 are devoted to cosmological parameters and weak lensing on the cosmological microwave background (CMB), respectively. Conclusions and future prospects are discussed in the last section.

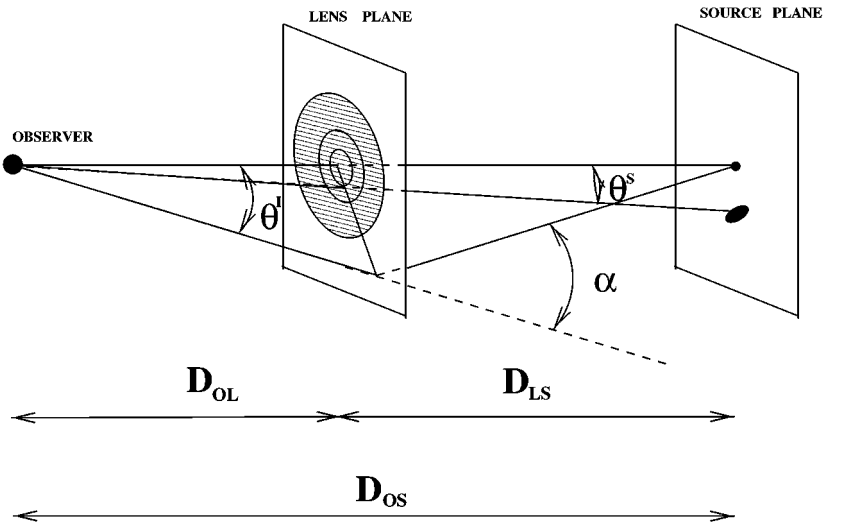

Figure 1 Description of a lensing configuration.

2. DEFINITIONS

2.1 Lensing Equations

In this preliminary section, I do not discuss at length the theoretical basis of the gravitational lens effect because all the details can be found in the comprehensive textbook written by Schneider et al (1992). I focus on concepts and basic equations of the gravitational lensing theory, in the thin lens approximation and for small deviation angles, which are necessary for this review.

The apparent angular position of a lensed image, $\boldsymbol{\theta}^I$ (in this review, bold symbols denote vectors), can be expressed as a function of the (unlensed) angular position of the source, $\boldsymbol{\theta}^S$, and the deflection angle, $\boldsymbol{\alpha}(\boldsymbol{\theta}^I)$ as follows (see Figure 1):

$$\boldsymbol{\theta}^I = \boldsymbol{\theta}^S + \frac{D_{LS}}{D_{OS}}\,\boldsymbol{\alpha}(\boldsymbol{\theta}^I). \tag{1}$$

$\boldsymbol{\alpha}(\boldsymbol{\theta}^I)$. depends on the projected mass density of the lens, $\Sigma(\boldsymbol{\theta}^I)$, and the cosmological parameters through the angular-diameter distances from the lens L to the source S, D_{LS}, from the observer o to the source, D_{OS}, and from the observer to the lens, D_{OL}:

$$\boldsymbol{\alpha}(\boldsymbol{\theta}^I) = \frac{4\pi G}{c^2} D_{OL} \frac{1}{\pi} \int \Sigma(\boldsymbol{\theta}^I) \frac{\boldsymbol{\theta}^I - \boldsymbol{\theta}'}{|\boldsymbol{\theta}^I - \boldsymbol{\theta}'|^2}\, d^2\theta', \tag{2}$$

where G is the gravitational constant and c is the speed of light. $\Sigma(\boldsymbol{\theta}^I)$ can be expressed as a function of the Poisson equation, and the strength of the lens is

characterized by the ratio of the projected mass density of the lens to its critical projected mass density Σ_{crit} (see Fort & Mellier 1994):

$$\frac{\Sigma(\boldsymbol{\theta}^I)}{\Sigma_{crit}} = \frac{4\pi G}{c^2}\frac{D_{LS}D_{OL}}{D_{OS}}\Sigma(\boldsymbol{\theta}^I) = \frac{1}{2}\Delta\varphi(\boldsymbol{\theta}^I), \tag{3}$$

where Δ is the 2-dimension Laplacian and φ is the dimensionless gravitational potential projected along the line of sight which is related to the projected gravitational potential Φ as follows:

$$\varphi = \frac{2}{c^2}\frac{D_{LS}D_{OL}}{D_{OS}}\Phi. \tag{4}$$

From the differentiation of Equation (1), we can express the deformation of an infinitesimal ray bundle as a function of the Jacobian

$$\frac{d\boldsymbol{\theta}^S}{d\boldsymbol{\theta}^I} = A(\boldsymbol{\theta}^I), \tag{5}$$

where $A(\boldsymbol{\theta}^I)$ is the *magnification matrix*:

$$A = \begin{pmatrix} 1-\partial_{11}\varphi & \partial_{12}\varphi \\ \partial_{12}\varphi & 1-\partial_{22}\varphi \end{pmatrix}. \tag{6}$$

It can be written as a function of two parameters (similar to the magnification and the astigmatism terms in classical optics), the *convergence*, κ, and the *shear* components γ_1 and γ_2 of the complex shear $\boldsymbol{\gamma} = \gamma_1 + i\gamma_2$:

$$A = \begin{pmatrix} 1-\kappa-\gamma_1 & \gamma_2 \\ \gamma_2 & 1-\kappa+\gamma_1 \end{pmatrix}. \tag{7}$$

The isotropic component of the magnification, $\kappa = 1/2\Delta\varphi(\boldsymbol{\theta}^I)$, is directly related to the projected mass density, and the two components γ_1 and γ_2 describe an anisotropic deformation produced by the tidal gravitational field. The eigenvalues of the magnification matrix are $1-\kappa\pm|\boldsymbol{\gamma}|$, where $|\boldsymbol{\gamma}| = \sqrt{\gamma_1^2+\gamma_2^2}$. They provide the elongation and the orientation produced on the images of lensed sources. The magnification of an image is:

$$\mu = \frac{1}{det(A)} = \frac{1}{(1-\kappa)^2+|\boldsymbol{\gamma}|^2}. \tag{8}$$

The points of the image plane where $det(A) = 0$ are called the critical lines. The corresponding points of the source plane are called the caustic lines and produce infinite magnification (see Schneider et al 1992; Blandford & Narayan 1992; Fort & Mellier 1994 for more detailed descriptions of caustic and critical lines). The strong lensing cases correspond to configurations where sources are close to the caustic lines. These lenses have $\Sigma(\boldsymbol{\theta}^I)/\Sigma_{crit} \geq 1$ and the convergence and shear are strong enough to produce giant arcs and multiple images for suitably positioned sources (Figures 2 and 3). The weak lensing regime,

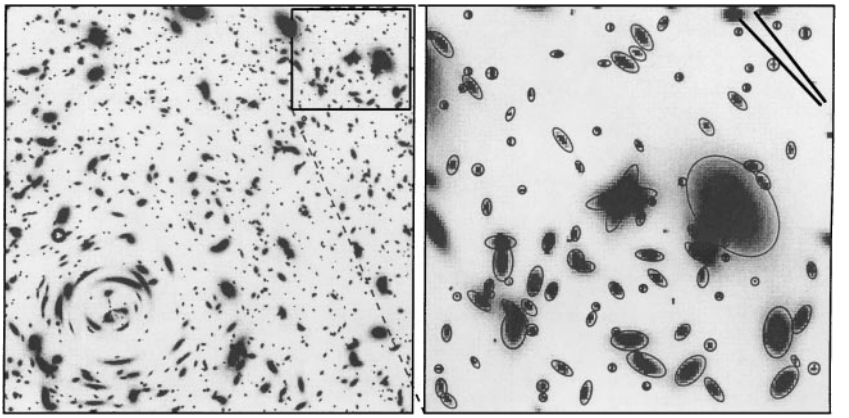

Figure 2 Illustration of the two lensing regimes. The left panel is a simulation of a cluster of galaxies at redshift 0.15, modeled by an isothermal sphere with a velocity dispersion of 1300 kms^{-1}. The lensed population has an average redshift of one. In the innermost region (*bottom left part of the panel*), tangential and radial arcs are clearly identified. As the radial distance of lensed galaxies increases, the shear decreases, and far from the cluster center, the ellipticity produced by the shear is lower than the intrinsinc ellipticity of the galaxies. The lensing signal must be averaged over a large number of galaxies in order to be measured accurately. The zoom on the right panel shows the images of the galaxies in the weak lensing regime. The contours show their shape as determined from their second moments. The average orientation of these galaxies is given by the solid lines at the top right. The lower line is the true orientation of the shear produced by the cluster at that position and the upper line is the orientation computed from 92 galaxies of the zoomed area. The difference between the two orientations is random noise due to the intrinsinc ellipticity and orientation distributions of the galaxies.

which is the main topic of this review, corresponds to lensing configurations where $\kappa \ll 1$ and $|\gamma| \ll 1$. In this regime, the magnification and the distortion of background galaxies are so small that they cannot be detected on individual objects. In that case, it is necessary to analyze statistically the distortion of the lensed population.

2.2 Relation with Observable Quantities

Let us assume that, to first approximation, faint galaxies can be described as ellipses. Their shape can be expressed as a function of their weighted second moments which fully define the properties of an ellipse,

$$M_{ij} = \frac{\int S(\boldsymbol{\theta})\left(\theta_i - \theta_i^C\right)\left(\theta_j - \theta_j^C\right) d^2\theta}{\int S(\boldsymbol{\theta}) 2\theta}, \tag{9}$$

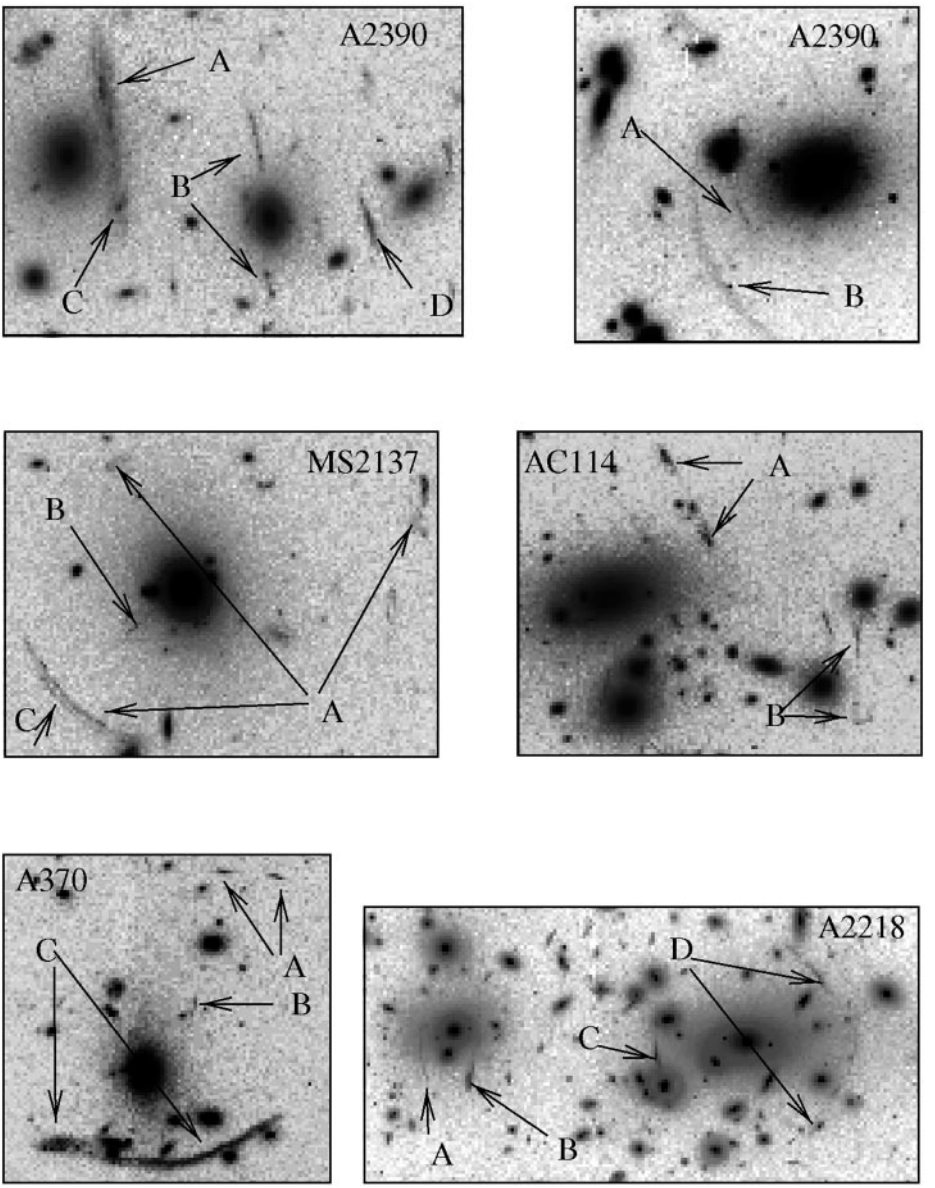

Figure 3 A panel of lensing clusters observed with HST. The arc(let)s and multiple lensed images are indicated by a letter. In A2390 (*top left*), the straight arc is made of two different galaxies corresponding to images A and C. The pairing of some images is obvious, like B in A2390 (*top-left*), A in AC114, or A in A370. Image B in MS2137 and B in A370 are radial arcs. A in MS2137 is a triple image from an almost ideal configuration of a fold caustic.

where the subscripts $i\,j$ denote the axes (1, 2) of coordinates θ in the source and the image planes, $S(\boldsymbol{\theta})$ is the surface brightness of the source and $\boldsymbol{\theta}^C$ is the center of the source.

Since the surface brightness of the source is conserved through the gravitational lensing effect (Etherington 1933), it is easy to show that, if one assumes that the magnification matrix is constant across the image (lensed source), the relation between the shape of the source, M^S and the lensed image, M^I is

$$M^I = A^{-1} M^S A^{-1}. \tag{10}$$

Therefore, to first approximation, the gravitational lensing effect on a circular source changes its size (magnification) and transforms it into an ellipse (distortion) with axis ratio given by the ratio of the two eigenvalues of the magnification matrix. The shape of the lensed galaxies can then provide information about these quantities. The approximation that the magnification matrix is constant over the image area is always valid in the weak-lensing regime, because the spatial scale variation of the magnification is much larger than the typical size of the lensed galaxies (a few arcseconds). This is not the case when the magnification tends to infinity, but this case is beyond the scope of this review (see Schneider et al 1992 and Fort & Mellier 1994).

The relation between the lens quantities described in Section 2.1 and the shape parameters of lensed galaxies is not immediately apparent. Although γ_1 and γ_2 describe the anisotropic distortion of the magnification, they are not directly related to observables (except in the weak-shear regime). It is preferable to use the *reduced complex shear*, $\mathbf{g}$, and the complex polarization (or distortion), $\boldsymbol{\delta}$, which is an observable,

$$\mathbf{g} = \frac{\gamma}{(1-\kappa)}; \quad \boldsymbol{\delta} = \frac{2g}{1+|\mathbf{g}|^2} = \frac{2\,\gamma(1-\kappa)}{(1-\kappa)^2+|\gamma|^2}, \tag{11}$$

because $\boldsymbol{\delta}$ can be expressed in terms of the observed major and minor axes a^I and b^I of the image, I, produced by a circular source S:

$$\frac{a^2-b^2}{a^2+b^2} = |\boldsymbol{\delta}|. \tag{12}$$

In this case, the two components of the complex polarization are easily expressed with the second moments:

$$\delta_1 = \frac{M_{11}-M_{22}}{Tr(M)}; \quad \delta_2 = \frac{2M_{12}}{Tr(M)}, \tag{13}$$

where $Tr(M)$ is the trace of the magnification matrix. For non-circular sources, from Equations (8) and (11) it is possible to relate the ellipticity of the image $\boldsymbol{\epsilon}^I$ to the ellipticity of the lensed source, $\boldsymbol{\epsilon}^S$. In the general case, it depends on the sign of $Det\,(A)$ (that is the position of the source with respect to the caustic lines) which expresses whether images are radially or tangentially elongated. In most cases of interest, $Det\,(A) > 0$ (the external regions, where the weak lensing regime applies) and:

$$\boldsymbol{\epsilon}^I = \frac{1+b^I/a^I}{1+b^I/a^I} e^{2i\vartheta} = \frac{\boldsymbol{\epsilon}^S + \mathbf{g}}{1-\mathbf{g}^*\,\boldsymbol{\epsilon}^S} \tag{14}$$

(Seitz & Schneider 1996), but when $Det(A) < 0$:

$$\boldsymbol{\epsilon}^I = \frac{1 + \boldsymbol{\epsilon}^{S*}\mathbf{g}}{\boldsymbol{\epsilon}^{S*} + \mathbf{g}^*}. \quad (15)$$

Equations 14 and 15 summarize most of the cases that will be discussed in this review.

3. MASS DISTRIBUTION IN CLUSTERS OF GALAXIES

3.1 Mass Reconstruction with Arclets

Recent Developments The use of arc(let)s and multiple images has already been discussed in detail in Fort & Mellier (1994). In the meantime, with the refurbishment of the HST, spectacular images of arc(let)s and multiply imaged galaxies have permitted enormous progress in this field. It turns out that giant arcs are no longer the strongest constraints on cluster mass distribution, because similar and even better information can be obtained with spatially resolved HST images of arclets.

The usual mass reconstruction technique with arc(let)s present in the innermost regions (close to the critical lines where arcs are located) is based on the assumption that the cluster mass density is smoothly distributed and can be expressed analytically, possibly with addition of some substructures, and on the hypothesis that the observed arc(let)s correspond to rather generic lens configurations, such as folds, cups or lisp caustics. These assumptions have already provided some convincing results with the use of ground-based images, in particular with predictions of the position of additional images (counter images) associated with arc(let)s (Hammer & Rigaud 1989; Mellier et al 1993; Kneib et al 1993, 1995). In all cases, it was found that the core radius of the dark matter distribution is small ($<50h_{100}^{-1}$ kpc) and that its geometry is compatible with the faint extended envelopes of light surrounding the giant cluster galaxies. The new investigations using the detailed morphology of the numerous arc(let)s visible in the HST images (see Figure 3) have provided more refined constraints on the dark matter distribution on the 100 kpc-scale (Hammer et al 1997, Gioia et al 1998, Kneib el al 1996, Tyson et al 1998). They confirm the trends inferred from previous ground-based data.

One critical issue concerning the approach described above is the possible sensitivity of the result to the analytical mass profile used for the modeling. Because none of the mass distribution has an unrealistic shape, the large-scale global property is expected to be well described. However, a direct comparison of the detailed mass distribution with theoretical expectations seen in simulations is difficult. Furthermore, the redshift distribution inferred from the lensing inversion (see section 5) can be strongly affected by the properties of the analytical model. AbdelSalam et al (1998a,b) have recently proposed a non-parametric mass reconstruction algorithm which helps to overcome the limitation of analytical modeling. The technique uses arc(let)s with known redshifts as strong constraints to recover a pixelised mass map of the lensing-cluster. The pixel-mass reconstruction uses the smoothed projected light distribution of the galaxy distribution which is then

pixelised exactly like the projected mass map. A fit of a pixelised Mass-to-Light ratio (M/L) permits one to relate the projected light distribution to the projected mass distribution for each pixel. The results found for A370 and A2218 (for A2218, weak and strong lensing features are used) are similar to those obtained otherwise, but this approach appears to be a very interesting alternative that permits a complete lens modeling based only on arc(let)s properties. Dye & Taylor (1998) attempted to generalize this approach in order to compute the convergence and the shear, in the weak lensing regime.

The X-ray/Lensing Mass Discrepancy The use of X-ray and optical images (ground-based or from the HST) of arc(let)s reveals that the X-ray peaks are located at the center of the most massive clumps of dark matter (Kneib et al 1995, Pierre et al 1996, AbdelSalam et al 1998a, Gioia et al 1998, Hammer et al 1997, Kneib el al 1996, Ota et al 1998, Kneib et al in preparation). On the other hand, the apparent contradiction between the mass estimated from X-ray data and the lensing mass ($M_{lensing} \approx 2$–$3\, M_X$), initially raised by Miralda-Escudé & Babul (1995), is not totally clear. The puzzling results obtained on several clusters, sometimes on the same cluster but analyzed by different groups, have not yet provided conclusive statements about the mass density profile and the X-ray versus dark matter dynamics. Böhringer et al (1998) find an excellent agreement between X-ray and lensing masses in A2390 which confirms the view claimed by Pierre et al (1996); Gioia et al (1998) show that the disagreement reaches a factor of 2 at least in MS0440+0204; Schindler et al (1997) find a factor of 2-3 discrepancy for the massive cluster RX 1347.4-1145, but Sahu et al (1998) claim that the disagreement is marginal and may not exist; Ota et al (1998) and Wu & Fang (1997) agree that there are important discrepancies in A370, Cl0500-24 and Cl2244-02.

As yet, there are no definitive interpretations of these contradictory results. It could be that the modeling of the gravitational mass from the X-ray distribution is not as simple. By comparing the geometry of the X-ray isophotes of A2218 to the mass isodensity contours of the reconstruction, Kneib et al (1995) found significant discrepancies in the innermost parts. The numerous substructures visible in the X-ray image have orientations which do not follow the projected mass density. They interpret these features as shocks produced by the infalling X-ray gas, which implies that the current description of the dynamical stage of the inner X-ray gas is oversimplified (see Markevitch 1997 and Girardi et al 1997 for similar views). Recent ASCA observations of three lensing-clusters corroborate the view that substructures are the major source of uncertainties (Ota et al 1998).

To study this possibility in more detail, Smail et al (1997a) and Allen (1998) have performed a detailed comparison between the lensing mass and X-ray mass for a significant number of lensing clusters. Both works conclude that the substructures have a significant impact on the estimate of X-ray mass. More remarkably, the X-ray clusters where cooling flows are present do not show a significant discrepancy with X-ray mass, whereas other X-ray clusters do (Allen 1998). This confirms that the discrepancy is certainly due to wrong assumptions on the physical state of

the gas. These two studies provide strong presumptions that we are now close to understanding the origin of the X-ray and lensing discrepancy.

An alternative has been suggested by Navarro et al (1997) who proposed that the analytical models currently used for modeling mass distributions may be inappropriate. Instead, they argue that the universal profile of the mass distribution produced in numerical simulations of hierarchical clustering may reconcile the lensing and X-ray masses. This is an attractive possibility because the universal profile is a natural outcome from the simulations that do not use external prescriptions. However, Bartelmann (1996) emphasized that the caustics produced by the universal profile predict that radial arcs should be thicker than observed in MS2137-23 (Fort et al 1992; Mellier et al 1994; Hammer et al 1997) and in A370 (Smail et al 1995b), unless the sources are very thin ($\approx$0.6 arcsecond for MS2137-23). This is not a strong argument against the universal profile because this is possible in view of the shapes of some faint galaxies observed with HST that some distant galaxies are indeed very thin. However, it is surprising that no radial arcs produced by "thick galaxies" have been detected so far. Even a selection bias would probably favor the observation of large sources rather than small, thin and hardly visible ones. Evans & Wilkinson (1998) have explored the range of slopes of cusp-like mass profiles which would produce radial arcs with thicknesses similar to those observed. As found by Bartelmann, they too found that the universal profile does not work well, but that a more singular mass profile could be satisfactory. They do not mention, however, whether these new profiles are compatible with the numerical simulations of Navarro et al (1997).

Probing the Clumpiness of Clusters HST images have also revealed the clumpiness of the cluster mass distribution on small scales. Although most of the HST images of lensing-clusters show arc(let)s with a coherent polarization on scales of 100 kpc, numerous perturbations are visible on scales of about 10 kpc. The long-range pattern is disrupted around most of the bright galaxies and shows saddle-shaped configurations as expected for clumpy mass distributions. In some extreme cases, giant arcs appear as broken filaments, probably disrupted by the halos around the brightest galaxies. With so much detail, one can therefore make a full mass reconstruction which takes into account all these clumps and possibly constrains the mass of individual cluster galaxies. For giant arcs, this has already been stressed by Kassiola et al (1992a), Mellier et al (1993), Kneib et al (1993), Dressler et al (1994), Wallington et al (1995) and Kneib et al (1996). They used the breaks (or the absence of breaks) in arcs to put upper limits to the masses of a few cluster galaxies which are superimposed on the arcs. The masses found for these cluster galaxies range between 10^{10} $M_\odot$ and 2×10^{11} $M_\odot$, with typical mass-to-light ratios between 5 and 15.

With the details visible on the HST images of arclets in A2218, AC114 or A2390, the sample of halos which can be constrained by this method is much larger and can provide more significant results. The number of details also permits use of more sophisticated methods of investigation. The most recent procedure uses the galaxy-galaxy lensing analysis. This technique is described in Section 5, but

because the clumpiness of dark matter in clusters is strongly related to the halos of cluster galaxies, I present the use of galaxy-galaxy lensing for cluster galaxies in this section.

The simplest strategy is to start with an analytical potential that reproduces the general features of the shear pattern of HST images, and in a second step, to include analytical halos around the brightest cluster members in the model. In practice, additional mass components are put in the model in order to interpret the arc(let)s which cannot be easily explained by the simple mass distribution. Some guesses are made in order to pair unexplained multiple images. The colors of the arc(let)s as well as their morphology help to make these associations. This approach was proposed by Natarajan & Kneib (1997), and Natarajan et al (1998). The detailed study done in AC114 by Natarajan et al indicates that about 10% of the dark matter is associated with halos of cluster galaxies. These halos have truncation radii smaller than field galaxies ($r_t \approx 15$ kpc) with a general trend of S0-galaxies to be even more truncated than the other galaxies. If this result is confirmed, it would be a direct evidence that truncation by tidal stripping is very efficient in rich clusters of galaxies. This result is somewhat contradictory with the absence of a clear decrease of rotation curves of spiral galaxies in nearby clusters (Amram et al 1993) which is interpreted as a proof that massive halos of galaxies still exist in cluster galaxies. However, it could be explained if the spirals that have been analyzed only appear to be in the cluster center because of projection effects, but actually are not located in the very dense region of the clusters where stripping is efficient.

Geiger & Schneider (1998, 1999) used a maximum likelihood analysis that explores simultaneously the distortions induced by the cluster as a whole and by its individual galaxies. They applied this analysis to the HST data of Cl0939+4713 and reached conclusions similar to those of Natarajan et al (1998). Several issues limit the reliability of their analyses and of the other methods as well (Geiger & Schneider 1998). First, depending on the slope of the mass profile of the cluster, the contributions of the cluster mass density and of the cluster galaxies may be difficult to separate. Second, it is necessary to have a realistic model for the redshift distribution of the background and foreground galaxies. Finally, the mass sheet degeneracy (see Section 3.2) is also an additional source of uncertainties. Regarding these limitations, Geiger & Schneider discuss the capability of the galaxy-galaxy lensing in clusters to provide valuable constraints on the galactic halos from the data they have in hand. Indeed, some of the issues they raised can be solved, such as the redshift distribution of the lensed galaxies. It would be interesting to take a more detailed look at how the analysis could be improved with more and better data.

3.2 Mass Reconstruction from Weak Lensing

A powerful and complementary way to recover the mass distribution of lenses has been proposed by Kaiser & Squires (1993). It is based on the distribution of weakly

lensed galaxies rather than the use of giant arcs. In 1988, Fort et al (1988) obtained at CFHT deep sub-arcsecond images of the lensing-cluster A370 and observed the first weakly distorted galaxies ever detected. The galaxy number density of their observation was about 30 arcmin^{-2}, mostly composed of background sources, far beyond the cluster. These galaxies lensed by the cluster show a correlated distribution of ellipticity/orientation which maps the projected mass density. The first attempt to use this distribution of arclets as a probe of dark matter was made by Tyson et al (1990), but the theoretical ground and a rigorous inversion technique was first proposed by Kaiser & Squires.

By combining Equations 2, 4, and 5, one can express the complex shear as a function of the convergence, κ (see Seitz & Schneider 1996 and references therein):

$$\gamma(\boldsymbol{\theta}) = \frac{1}{\pi} \int \mathcal{D}(\boldsymbol{\theta} - \boldsymbol{\theta}')\, \kappa(\boldsymbol{\theta}')\, d^2\theta', \tag{16}$$

where

$$\mathcal{D}(\boldsymbol{\theta} - \boldsymbol{\theta}') = \frac{\left(\theta_2 - \theta_2'\right)^2 - \left(\theta_1 - \theta_1'\right)^2 + 2i\left(\theta_1 - \theta_1'\right)\left(\theta_2 - \theta_2'\right)}{|(\boldsymbol{\theta} - \boldsymbol{\theta}')|^4}. \tag{17}$$

This equation can be inverted in order to express the projected mass density, or equivalently κ, as function of the shear:

$$\kappa(\boldsymbol{\theta}) = \frac{1}{\pi} \int \Re[\mathcal{D}^*(\boldsymbol{\theta} - \boldsymbol{\theta}')\, \gamma(\boldsymbol{\theta}')]\, d^2\theta' \; + \kappa_0, \tag{18}$$

where $\Re$ denotes the real part. From Equation 14 we can express the shear as a function of the complex ellipticity. Hence, if the background ellipticity distribution is randomly distributed, then $\langle |\epsilon^S| \rangle = 0$ and

$$\langle |\epsilon^I| \rangle = |\mathbf{g}| = \frac{|\gamma|}{1 - \kappa}, \tag{19}$$

(Schramm & Kayser 1995). In the most extreme case, when $\kappa \ll 1$ (the linear regime discussed initially by Kaiser & Squires 1993), $\langle |\epsilon^I| \rangle \approx |\gamma|$, and therefore, the projected mass density can be recovered directly from the measurement of the ellipticities of the lensed galaxies.

The first cluster mass reconstructions using the Kaiser & Squires linear inversion have been done by Smail (1993) and Fahlman et al (1994). Fahlman et al estimated the total mass within a circular radius using the *Aperture densitometry* technique (or the "ζ-*statistics*"), which consists of computing the difference between the mean projected mass densities within a radius r_1 and within an annulus $(r_2 - r_1)$ (Fahlman et al 1994, Kaiser 1995) as function of the *tangential shear*, $\gamma_t = \gamma_1 \cos(2\vartheta) + \gamma_2 \sin(2\vartheta)$ (see Equation 14), averaged in the ring:

$$\zeta(r_1, r_2) \;=\; \langle \kappa(r_1) \rangle - \langle \kappa(r_1, r_2) \rangle \;=\; \frac{2}{1 - r_1^2/r_2^2} \int_{r_1}^{r_2} \langle \gamma_t \rangle\, d\ln r. \tag{20}$$

TABLE 1 Main results obtained from weak lensing analyses of lensing-clusters. The scale is the typical radial distance with respect to the cluster center. The last cluster has two values for the M/L ratio. This corresponds to two extreme redshifts assumed for the lensed population, either $z = 3$ or $z = 1.5$. For this case, the two values given for the velocity dispersion are those inferred when $z = 3$ or $z = 1.5$ are used.

Cluster	z	σ_{obs} (kms^{-1})	σ_{wl} (kms^{-1})	M/L (h_{100})	Scale (h_{100}^{-1} Mpc)	Tel.	Ref.
A2218	0.17	1370	—	310	0.1	HST	Smail et al (1997)
A1689	0.18	2400	1200–1500	—	0.5	CTIO	Tyson et al (1990)
			—	400	1.0	CTIO	Tyson & Fischer (1995)
A2163	0.20	1680	740–1000	300	0.5	CFHT	Squires et al (1997)
A2390	0.23	1090	≈1000	320	0.5	CFHT	Squires et al (1996b)
Cl1455+22	0.26	≈700	—	1080	0.4	WHT	Smail et al (1995)
AC118	0.31	1950	—	370	0.15	HST	Smail et al (1997)
Cl1358+62	0.33	910	780	180	0.75	HST	Hoekstra et al (1998)
MS1224+20	0.33	770	—	≈800	1.0	CFHT	Fahlman et al (1994)
Q0957+56	0.36	715	—	—	0.5	CFHT	Fischer et al (1997)
Cl0024+17	0.39	1250	—	150	0.15	HST	Smail et al (1997)
			1300	≈900	1.5	CFHT	Bonnet et al (1994)
Cl0939+47	0.41	1080	—	120	0.2	HST	Smail et al (1997)
			—	≈250	0.2	HST	Seitz et al (1996)
Cl0302+17	0.42	1080		80	0.2	HST	Smail et al (1997)
RXJ1347−11	0.45	—	1500	400	1.0	CTIO	Fischer & Tyson (1997)
3C295	0.46	1670	1100–1500	—	0.5	CFHT	Tyson et al (1990)
			—	330	0.2	HST	Smail et al (1997)
Cl0412-65	0.51	—	—	70	0.2	HST	Smail et al (1997)
Cl1601+43	0.54	1170	—	190	0.2	HST	Smail et al (1997)
Cl0016+16	0.55	1700	—	180	0.2	HST	Smail et al (1997)
			740	740	0.6	WHT	Smail et al (1993)
Cl0054-27	0.56	—	—	400	0.2	HST	Smail et al (1997)
MS1137+60	0.78	859[1]	—	270	0.5	Keck	Clowe et al (1998)
RXJ1716+67	0.81	1522[2]	—	190	0.5	Keck	Clowe et al (1998)
MS1054-03	0.83	1360[3]	1100–2200	350–1600	0.5	UH2.2	Luppino & Kaiser (1997)

[1]Gioia, private communication.

[2]Gioia et al (1998).

[3]Donahue et al (1998).

This quite robust mass estimator minimizes the contamination by foreground and cluster galaxies and permits a simple check that the signal is produced by shear, simply by changing γ_1 in γ_2 and γ_2 in $-\gamma_1$ which should cancel out the true shear signal.

The mass maps inferred from their images coincide with the light distribution from the galaxies. But, the impressive M/L found in the lensing cluster MS1224+20 by Fahlman et al (see Table 1) led to a surprisingly high value of Ω (close to 2!). This result is somewhat questionable and is probably due to the various sources of errors, possibly in the correction of PSF anisotropy (see Section 3.3). Furthermore, the two-dimensional mass reconstructions presented in the

earliest papers looked noisy, probably because of boundary effects from the intrinsically non-local reconstruction, the geometry of the finite-size charge coupled device (CCD), and the reconstruction algorithm that can have terrible effects on the inversion. These problems have been discussed in several papers (Schneider & Seitz 1995, Seitz & Schneider 1995a, Schneider 1995, Seitz & Schneider 1996). In particular, Kaiser (1995) and Seitz & Schneider (1996) generalized the inversion to the non-linear regime, by solving the integral equation obtained from Equation 18 by replacing γ by $(1-\kappa)\mathbf{g}$, or similarly by using the fact that both κ and γ depend on second derivatives of the projected gravitational potential φ (Kaiser 1995) which permits one to recover the mass density by this alternative relation:

$$\nabla \log(1-\kappa) = \frac{1}{1-|\mathbf{g}|^2} \cdot \begin{pmatrix} 1+g_1 & g_2 \\ g_2 & 1-g_1 \end{pmatrix} \begin{pmatrix} \partial_1 g_1 + \partial_2 g_2 \\ \partial_1 g_2 - \partial_2 g_1 \end{pmatrix}. \qquad (21)$$

Both Equations 18 and 21 express the same relation between κ and γ and can be used to reconstruct the projected mass density. The improvements that have been proposed and discussed in detail by Seitz & Schneider (1995a), Kaiser (1995), Schneider (1995), Bartelmann (1995c), Squires & Kaiser (1996), Seitz & Schneider (1996, 1997) and Lombardi & Bertin (1998a,b) lead to reliable mass reconstructions from lensing inversion, and comparison with simulated clusters proves that it can now be considered a robust technique (see Figure 4, in particular the comparision between Figure 4a, and Figures 4g and 4h). However, the recovered mass distribution is not unique because the addition of a lens plane with constant mass density will not change the distortion of the galaxies (see Equation 18). Furthermore, the inversion only uses the ellipticity of the galaxies without regard to their dimension, so that changing $(1-\kappa)$ in $\lambda(1-\kappa)$ and γ in $\lambda\ \gamma$ keeps $\mathbf{g}$ invariant. This so-called *mass sheet degeneracy* initially reported by Gorenstein et al (1988), has been pointed out by Schneider & Seitz (1995) as a fundamental limitation of the lensing inversion.

The degeneracy could in principle be broken if the magnification can be measured independently, because it is not invariant under the linear transformation mentioned above, but instead it is reduced by a factor of $1/\lambda^2$. Broadhurst et al (1995) proposed measuring the magnification directly by using the magnification bias which changes the galaxy number-counts (see Section 3.4), whereas Bartelmann & Narayan (1995) explored their *lens parallax method* which compares the angular sizes of lensed galaxies with an unlensed sample. The lens-parallax method requires a sample of unlensed population having the same surface brightness distribution. However, in the case of ground-based observations, for the faintest (i.e. smallest galaxies), the convolution of the signal by the seeing disk can significantly affect the measurement of their surface brightness. Therefore, the method requires a careful handling of small-sized objects. A more promising approach is the use of wide field cameras with a typical field of view much larger than clusters of galaxies. In that case κ should vanish at the boundaries of the field, so that the degeneracy could in principle be broken.

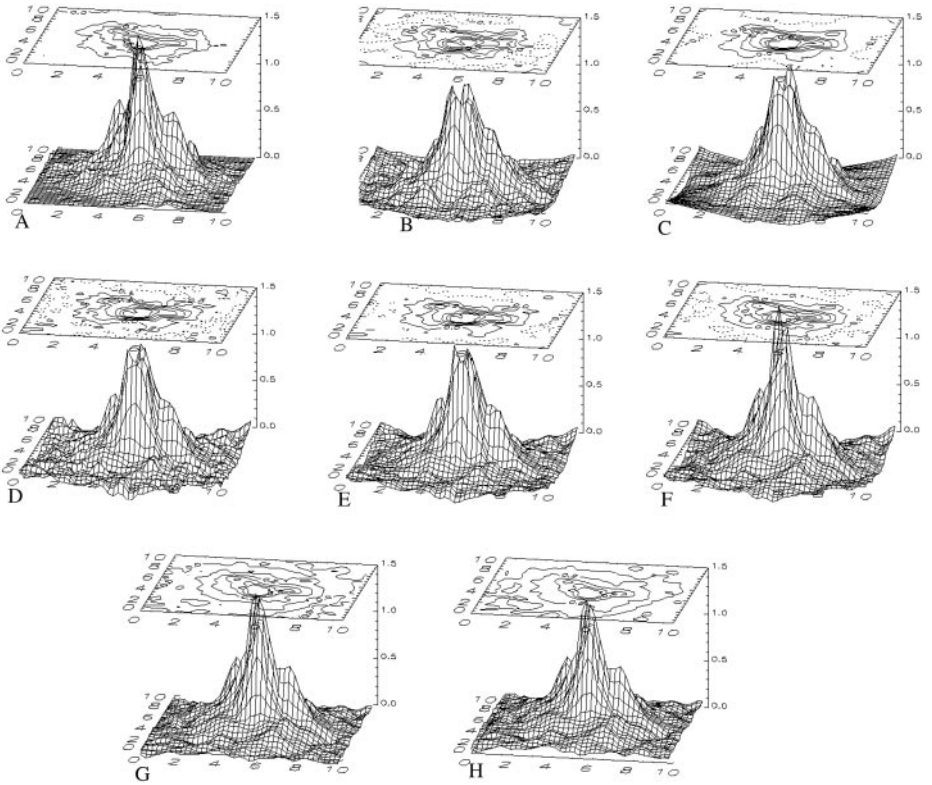

Figure 4 Examples of different algorithms for the mass reconstruction of clusters. Image A (*top left*) is the original simulated lensing cluster. Panel B shows an original Kaiser & Squires (1993) mass reconstruction, assuming that all background sources are circular. Panel C shows the same reconstruction as panel B, but with another smoothing method, which was proposed by Seitz & Schneider (1995a), in order to smooth the distortion distribution. Panel D shows the same result but the sources have an ellipticity distribution. Panel E shows the same reconstruction as panel D, but uses an adaptive smoothing scale. In panel F the linear and non-linear weak lensing regimes are now used in the inversion. Panel G shows the same reconstruction algorithm as F, with an additional extrapolation of the distortion field outside the field. The last panel shows the mass reconstruction with the constraint that the minimal mass density at any point is zero (from Seitz & Schneider 1995a).

An attractive alternative has been suggested by Bartelmann et al (1996) who proposed a maximum likelihood reconstruction algorithm. The advantage is that this is a *local* approach because it fits the projected potential at each grid-point. The observables are constrained by the second-derivatives of the potential, using a least-χ^2 which simultaneously computes both the magnification and the distortion, which are compared to the ellipticity and the sizes of the galaxies. Squires & Kaiser (1996) and Bridle et al (1998) have investigated similar maximum-likelihood techniques with different regularizations, though they fit the projected mass density rather than the potential. It seems however more attractive to use the deflection potential rather than the projected mass distribution in order to avoid incomplete knowledge of the contribution to the projected mass density of the matter outside the observed area (Seitz et al 1998).

The comparison done by Squires & Kaiser (1996) between the *direct reconstructions*, like the Kaiser & Squires (1993) approach, and the *inversion methods*, like the maximum likelihood reconstructions, did not lead to conclusive results, though the maximum likelihood inversion looks somewhat better. It is worth pointing out that one of the advantages of the maximum likelihood inversion is that it eases the addition of some observational constraints, such as strong lensing features (Bartelmann et al 1996; Seitz et al 1998). More recently, Seitz et al (1998) proposed an improved entropy-regularized maximum-likelihood inversion in which they no longer smooth the data, but instead use the ellipticity of each individual galaxy.

Since 1990, many clusters have been investigated using the weak lensing inversion, using either ground-based or HST data that are summarized in Table 1, but the comparison of these results is not straightforward because of the different observing conditions which produced each set of data and the different mass reconstruction algorithms used by each author. Nevertheless, all these studies show that on scales of about 1 Mpc, the geometry of mass distributions, the X-ray distribution and the galaxy distribution are similar (see Figure 5), although the ratio of each component compared with the others may vary with radius. The inferred M/L ratio lies between $100h_{100}$ to $1600h_{100}$, with a median value of approximately $300h_{100}$, with a trend to increase with radius. Contrary to the strong lensing cases, there is no evidence of discrepancies between the X-ray mass and the weak lensing mass. It is worth noting that the strong-lensing mass and the weak-lensing mass estimates are consistent in the region where the amplitudes of two regimes are very close. This is an indication that the description of the X-ray gas, and its coupling with the dark matter on the scales corresponding to strong-lensing studies, is oversimplified, whereas on larger scales, described by weak-lensing analysis, the detailed description of the gas has no strong impact.

The large range of M/L could partly be a result of one of the issues of the mass reconstruction from weak lensing. As shown in Equation 1, the deviation angle depends on the ratios of the three angular-diameter distances, which vary with the redshift assumed for the sources. For low-z lenses, the dependence with redshift of the background galaxies is not considerable, so the calibration of the mass can

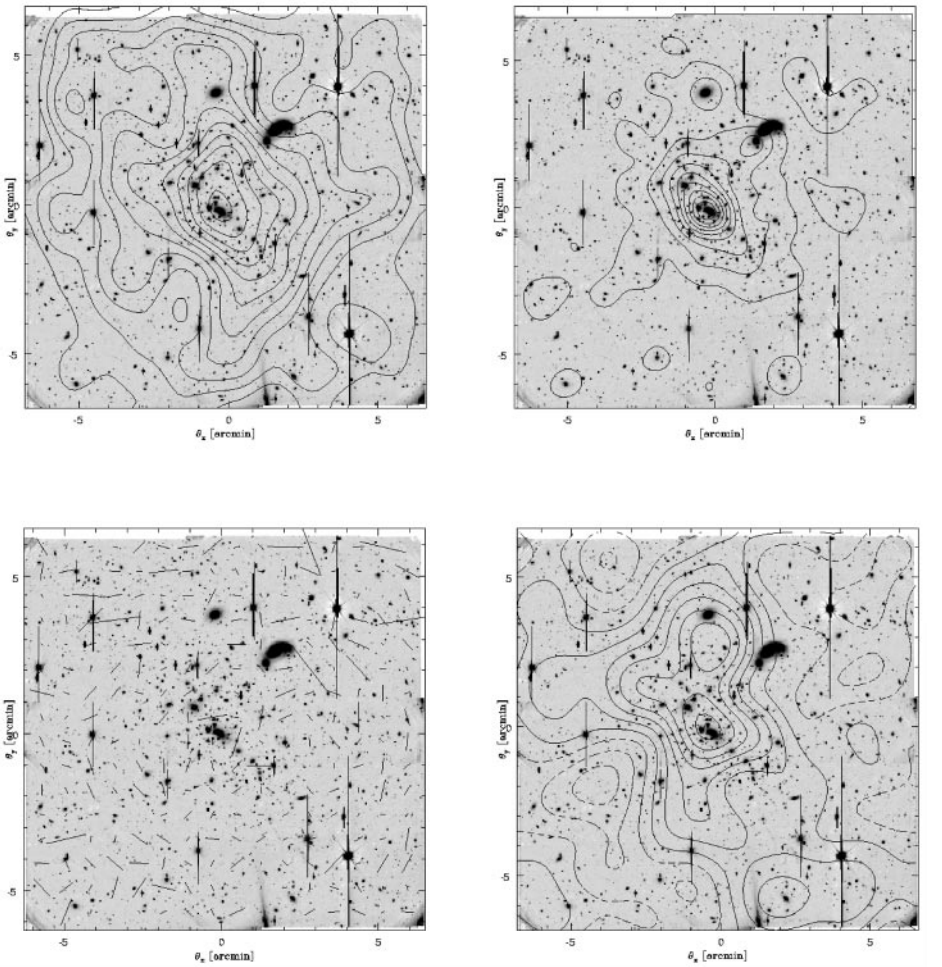

Figure 5 Weak lensing analysis and mass reconstruction of A2218 (from Squires et al 1996a). The images have been obtained at CFHT in I-band. The *top-left* panel shows the smoothed galaxy number density and the *top-right* shows the smoothed light distribution. The *bottom-left* is the shear map. The length of each line is proportional to the amplitude of the shear. From this shear map, the mass reconstruction of the Kaiser & Squires (1993) algorithm produces the mass map on the *bottom-right*. The correlation between the light and the matter distribution is clear.

be provided with a reasonable confidence level. However, distant clusters are highly sensitive to the redshift of the sources, and it becomes very difficult to scale the total mass without this information, even though the shape of the projected mass density is reconstructed correctly. The case of high-redshift clusters is more complicated. For a low-z cluster (say $z < 0.4$), it is not necessary to go extremely deep since the background galaxies are between $z = 0.4$ to 1. Thus, spectroscopic surveys can provide the redshift distribution with a good accuracy. In contrast, the background sources lensed by high-z clusters are beyond $z = 1$ and therefore are dominated by very faint galaxies ($I > 22.5$) which cannot be observed easily by spectroscopy.

The masses inferred from the strong lensing and weak lensing reconstruction put valuable constraints on the median M/L of lensing clusters. From the investigation of about 20 clusters, the median M/L is lower than $400h_{100}$. This implies that weak lensing analyses predict $\Omega < 0.3$ with a high significance level. Even if the uncertainties are large and if the weak lensing inversion needs to be improved, the HST data, in particular for clusters with giant arcs and many arc(let)s with known redshift, imply that the mass of clusters of galaxies cannot be reconciled with an Einstein-de Sitter (EdS) universe. The constraints on Ω are in good agreement with other observations (see the recent discussion by Krauss 1998).

Another strong statement results from the mass reconstruction obtained by Luppino & Kaiser (1997) and Clowe et al (1998) or the detection of giant arcs in very distant clusters (Deltorn et al 1997): massive clusters do exist at redshift $\approx$1! Though the total mass and the M/L cannot be given with a high accuracy, it cannot change the conclusion, unless unknown important systematics have been neglected. Therefore, we now have the first direct observational evidences that high mass-density peaks have generated massive clusters of galaxies at redshift 1. These results are extremely promising and are corroborated by other weak lensing studies around radiosources and quasars (see Section 4.2). Indeed, because these studies question the standard Cold Dark Matter (CDM) model and instead favor low-density universes, we can certainly expect fantastic developments from the investigation of high-redshift clusters with weak lensing during the coming years.

The impressive and spectacular results obtained by weak-lensing have demonstrated the power of this technique. However, although the results seem reliable in the cluster center (say within 500 kpc), there are still uncertainties outward, where the shear becomes very small. A critical issue of the lensing inversion is the reliability of the mass reconstruction and how it degrades when the shear decreases. Kaiser (1995) emphasized that Equation 20 can be used as a check of the mass reconstruction since the curl of $\nabla \log(1 - \kappa)$ should be zero only if the shear is recovered properly. Van Waerbeke (1999) has recently proposed an elegant way to estimate the accuracy of the mass reconstruction from the noise properties of the reconstruction. Nevertheless, the comparison of results using different algorithms and the stability and the reproducibility of each inversion have still to be done in order to demonstrate that weak lensing analysis produces reliable results. This is important for the future, when ground-based observations of very large fields

will be performed. Mellier et al (1997) have compared the shear maps obtained in A1942 by using the Bonnet-Mellier and the autocorrelation function (ACF) methods (see next section). Though the two maps are similar, discrepancies are visible at the periphery, but no quantitative estimates of the similarity of both maps are given. An important step was taken by Van Waerbeke et al (in preparation) who analyzed A1942 using different shear measurements, different mass reconstruction algorithms and different data, obtained with two CCD cameras mounted at CFHT. Three sets of data have been used, all of them having a total exposure time of 4 hours and a seeing of $0.7''$. The results show impressive similarities even in the details of the mass reconstruction, down to a shear amplitude of 2%. This is the first work that demonstrates that results are stable and are not produced by artifacts, even at a very low shear amplitude. The main concerns are the capabilities of instruments, and the image analysis algorithms to measure very weak shear. This critical issue deserves a detailed discussion, which is the subject of the next section.

3.3 Measuring Weak Shear

In addition to the technical problem of the mass reconstruction algorithm and the redshift distribution of the sources, weak lensing is also sensitive to the accuracy of the measurement of ellipticities of lensed galaxies. The atmosphere has dramatic effects; in particular, the seeing circularizes the innermost part of galaxies which affects the measurements of shapes of faint galaxies (see for example the simulations by Bartelmann 1995c). These issues have been investigated in detail by Bonnet & Mellier (1995), Mould et al (1994), Kaiser et al (1995) and Van Waerbeke et al (1997). Atmospheric effects (seeing, atmospheric refraction, atmospheric dispersion), telescope handling (flexures of the telescopes, bad guiding) and optical distortions are extrinsic problems that can bias the measurements, though in principle they can be corrected in various ways. The atmospheric dispersion can be minimized by using an I-band filter and by observing clusters close to zenith, which also minimizes the flexures. Optical distortions can be corrected either analytically, if the optics are known perfectly, or by using the stars located in the fields. On the other hand, the ellipticity distribution of the galaxies is an intrinsic source of noise.

The extrinsic and intrinsic noises compete together: the circularization by the seeing is important only for the faint galaxies because their typical size is of the same order as the seeing disk. So, in principle it should be better to use only large (bright) galaxies, though they are not as numerous as the small (faint) galaxies. On the other hand, the noise produced by the intrinsic ellipticity distribution of the galaxies is minimized by averaging the shape of a large number of galaxies. The typical scale on which galaxies can be averaged is defined by the spatial resolution of the reconstructed mass map. For intermediate and high-redshift clusters of galaxies the typical angular scale is a few arcminutes, so that galaxies must be averaged on less than one arcminute in order to map the projected mass-density

with a good sampling. If we assume an ellipticity dispersion, σ_ε of about 0.3, as it is suggested by nearby surveys and the distribution of galaxies in the Hubble Deep Field (HDF), then we can measure an ellipticity, ϵ, produced by a gravitational shear of $|\gamma| = 10\%$ if the number of averaged galaxies, N is:

$$N > \left(\frac{\sigma_\varepsilon}{\epsilon}\right)^2 \approx 10. \tag{22}$$

It is therefore quite easy to measure gravitational shear of 10% on an arcminute scale. However, going down to 1% would require about 900 galaxies which is not feasible on such an angular scale, unless many fields of 1 arcminute are averaged. An alternative is to go deeper in order to increase the galaxy number density. However, this is not sufficient to increase the accuracy of the results, because most of the faint galaxies have an unknown redshift distribution which prevents scaling the mass properly, and also because it is difficult to correct them from PSF.

The procedure to recover the shear field from the ellipticities of individual galaxies has several solutions. Bonnet & Mellier (1995) compute the second moment of galaxies (see Equation 9) within a circular annulus and average the signal on a given area (a *superpixel*) by using only the faint galaxies that dominate their deep observations. The size of the inner radius is constant and close to the seeing disk, which minimizes the effect of the circularization of the innermost isophotes on the measurement of the ellipse. The outer radius is also constant and has been optimized by using simulations of galaxies in order to get the highest signal-to-noise ratio on each second moment. The drawback of this approach is that the second moment of this annulus is no longer a direct measurement of the shape of the galaxy and it must be calibrated by simulations for each observing condition. The anisotropy of the PSF is corrected on the averaged signal, assuming that it is dominated by optical defects and that it behaves like a stretching of the image. This assumption is not valid for individual galaxies, but for each superpixel, deep observations average so many galaxies that it is possible to assume that the resulting signal reflects the one produced by an ideal galaxy having the same profile on each superpixel. In this case, Bonnet & Mellier have shown from simulations that the correction works very well down to a shear amplitude of 3% (see Bonnet et al 1994, and Schneider et al 1998a).

Kaiser et al (1995) (see also Luppino & Kaiser 1997, Hoekstra et al 1998 for further developments) compute the second moment within a variable aperture which depends on the size of individual galaxies; however, instead of an annulus they use a Gaussian filter, and introduce a more rigorous correction of the PSF anisotropy. Because they do not make selection from the size of the galaxies to measure the shear, it is clear that the largest galaxies require less correction. Therefore their correction depends on the total area of each individual galaxy. Assuming that the anisotropy of the PSF is small, Kaiser et al introduced a smearing correction, defined by a linear smear polarizability which expresses the (small) shift of polarization of galaxies induced by an anisotropic PSF. To first order, this shift can be expressed analytically and provides the correction from the shapes of

the stars visible in the field, by dividing the smear polarizability by the observed polarization of stars. The efficiency of this method has been tested by using HST images which were degraded to the corresponding PSF anisotropy expected on ground-based images. They proved that the correction works very well. However, the method only works for bright galaxies. For fainter samples, they calibrated the polarization-shear relation by artificially lensing HST images and then by degrading them by the PSF observed in their data. However, it seems more preferable to calibrate the PSF anisotropy directly from the images. Luppino & Kaiser (1997) calibrated the anisotropic correction only from the observations of the stars in their fields, without auxiliary data.

Mould et al (1994) proposed a different procedure: they computed the second moment within a limiting isophote rather than a finite aperture and corrected linearly from the PSF anisotropy, assuming, as did Kaiser et al, that the correction is inversely proportional to the area of the source.

Van Waerbeke et al (1997) proposed an original alternative that fully exploits the signal down to the noise level on each CCD image and reduces the error of the second moment of galaxies. Instead of using individual objects, they compute the local auto-correlation function (ACF), $\xi(\boldsymbol{\theta})$, of pixels, averaged on a given area:

$$\xi(\boldsymbol{\theta}) = \langle (I(\boldsymbol{\theta}) - \langle I \rangle)\,(I(\boldsymbol{\theta} + \boldsymbol{\theta}') - \langle I \rangle) \rangle, \tag{23}$$

where $\langle I \rangle$ is the mean surface brightness of the area. The (unlensed) ACF of the averaged source population, ξ^S, is an isotropic quantity, which by definition is centered, and therefore does not depend on the detection procedure and on the computation algorithm of its centroid. When a lensing signal is present, the shape of the ACF of the lensed population, $\xi^I(\boldsymbol{\theta}) = \xi^S(A\boldsymbol{\theta})$ is no longer isotropic. For example, in the weak lensing regime:

$$\xi^I(\boldsymbol{\theta}) = \xi^S(|\boldsymbol{\theta}|) - |\boldsymbol{\theta}|\,\partial_{\boldsymbol{\theta}}\xi^S(|\boldsymbol{\theta}|)\;\;(I - A)\,, \tag{24}$$

where I is the identity matrix. The ACF is now composed of the unlensed isotropic component plus an anisotropic term which depends on the magnification matrix, A, which stretches it like a real object. The second moment of the ACF can also be expressed as a function of the distortion and the magnification (Van Waerbeke et al 1997). Because all the pixels of the image are used, the ACF uses the full information of the image; in particular, the flux coming from extremely faint objects, for which the measurement of a centroid and the second moments are not measurable precisely, is also taken into account. For that reason, in principle, the ACF can work on images that reach the confusion limit (Van Waerbeke et al 1997, Réfrégier & Brown 1998). It turns out that in practice it is better to use the ACF around detected galaxies than on the total image because correlated noises, such as electronics cross-talk or shift-and-add residuals, may generate spurious coherent signals (Van Waerbeke & Mellier 1997). This method looks ideal for the optimal extraction of weak lensing signals because the signal-to-noise ratio of the ACF is always high enough and spreads over sufficient pixels to avoid the need for circular

filtering, such as faint galaxies, and to provide an accurate estimate of its shape parameters.

The reliability of the relation between measured ellipticities and shear, and of the mass reconstruction obtained from observations, has been checked by Kaiser & Squires (1993) and Bonnet & Mellier (1995), and by the independent simulations of Bartelmann (1995c) and Wilson et al (1996a). Despite careful studies to check that images are corrected accurately from circularization by seeing and PSF anisotropy (in particular the spatial variation of the PSF in the field can be modeled), there is still a lot of work to do in this area. For instance, the weighting functions proposed to measure the ellipticities are based on intuition but no complete investigation has been done so far to find the optimal one. Moreover, for each of these procedures, it is assumed that the PSF anisotropy is unidirectional. This may not be true, in particular when instruments with poor optical design are used. In that case, the correction becomes non-trivial, and paradoxically this could appear on the image with the best image quality because details of the PSF are no longer smeared by circularization of the seeing. This domain is certainly at its infancy and much work and many new ideas should appear during the next years, mainly because the shear produced by large-scale structures is expected to be very small.

3.4 Mass Profile from the Magnification Bias

Parallel to the mass reconstruction using weak shear measurements, one can use the direct measurement of the magnification from the local modification of the galaxy number density. This "magnification bias" expresses the simultaneous effects of the gravitational magnification, which increases the flux received from any lensed galaxies and permits the detection of galaxies enhanced by the amplification, but also magnifies by the same amount the area of the projected lensed sky and thus decreases the apparent galaxy number density. The total amplitude of the magnification bias depends on the slope of the galaxy counts as a function of magnitude and on the magnification factor of the lens. For a circular lens, the radial galaxy number density of background galaxies writes:

$$N(<m,r) = N_0(<m)\,\mu(r)^{2.5\alpha-1} \approx N_0\,(1+2\kappa)^{2.5\alpha-1} \quad \text{if } \kappa \text{ and } |\gamma| \ll 1, \quad (25)$$

where $\mu(r)$ is the magnification, $N_0(<m)$ is the intrinsic (unlensed) number density, obtained from galaxy counts in a nearby empty field, and α is the intrinsic count slope:

$$\alpha = \frac{\mathrm{d}\log N(<m)}{\mathrm{d}m}. \quad (26)$$

A radial magnification bias $N(<m,r)$ shows up only when the slope $\alpha \neq 0.4$; otherwise, the increasing number of magnified sources is exactly compensated by the apparent field dilatation. For slopes larger than 0.4 the magnification bias increases the galaxy number density, whereas for slopes smaller than 0.4 the radial

density will show a depletion. Hence, no change in the galaxy number density can be observed for $B(<26)$ galaxies, since the slope is almost this critical value (Tyson 1988). However, it can be detected in the $B > 26$, $R > 24$ or $I > 24$ bands when the slopes are close to 0.3 (Smail et al 1995c).

The change of the galaxy number density can be used as a direct measurement of the magnification and can be included in the maximum likelihood inversion as a direct observable in order to break the mass sheet degeneracy (see Section 3.2). Alternatively, it can also be used to model the lens itself. In the case of a singular isothermal sphere, the magnification can be expressed as a function of the velocity dispersion of the lens, σ, and the radial distance $\theta = r/r_E$, where $r_E = 4\pi\sigma^2/c^2\ D_{LS}/D_{OS}$:

$$\mu(r) = \frac{4\pi\sigma^2}{c^2}\ \frac{D_{LS}}{D_{OS}}\ \frac{\theta}{\theta - 1}. \tag{27}$$

Reconstruction of cluster mass distribution using magnification bias was initially explored by Broadhurst et al (1995), and has been used by Taylor et al (1998) in A1689, and by Fort et al (1997) in Cl0024+1654 (see also a generalization by Van Kampen 1998). The masses found are consistent with those inferred from gravitational weak shear or from strong lensing.

This magnification bias is an attractive alternative to the weak shear because it is only based on the galaxy counts and does not require outstanding seeing to measure ellipticities and orientations of galaxies. However, it is more sensitive to shot noise, which unfortunately increases when the number density decreases in the depletion area. Furthermore, it also depends on the galaxy clustering of the background sources which can have large fluctuations from one cluster to another. Indeed, in the weak lensing regime, assuming that $\kappa \approx |\gamma|$, the ratio of the signal-to-noise ratios of the shear and the depletion, $R_{Sh/Dep}$, clearly favors the shear analysis:

$$R_{Sh/Dep} = \frac{|\gamma|}{\sigma_\varepsilon}\frac{1}{\kappa|(5\alpha - 2)|}\ \approx 3, \tag{28}$$

for a dispersion of the intrinsic ellipticity distribution of the galaxies, $\sigma_\varepsilon = 0.3$, and $\alpha = 0.2$. Despite these limitations, this is a simple way to check the consistency of the mass reconstruction. Its great merit is that it is not sensitive to systematic effects, such as the weak shear measurement which depends on the correction from the PSF of the observed ellipticities.

4. LARGE-SCALE STRUCTURES AND COSMIC SHEAR

The idea that mass condensations and the geometry of the Universe can alter light bundles and distort the images of distant galaxies was emphasized by Kristian & Sachs (1966), and later by Gunn (1967) and Blandford & Jaroszyński (1981), who first gave a quantitative estimate of the amplitude of this effect. Kristian

(1967) looked at this effect on photographic plates of six clusters of galaxies using the Palomar Telescope, but found nothing significant. Valdes et al (1983) were the first to attempt to measure a coherent alignment of distant galaxies generated by large-scale structures. They used about 40,000 randomly selected field galaxies with J magnitudes between 22.5 and 23.5, but, like Kristian, they did not find any conclusive signal. These negative measurements were not definitely interpreted as important cosmological constraints on the curvature and the mass distribution in our Universe, but instead as a result of technical limitations related to the poor image quality of the photographic data. Indeed, the recent weak lensing analysis produced by a supercluster candidate done by Kaiser et al (1998) seems to show that large-scale structures produce gravitational shear which is already detectable. Numerical simulations by Schneider & Weiss (1988) using point-mass models, or by Babul & Lee (1991) using a smooth mass distribution, showed that both the ellipticity distribution and the apparent luminosity function of distant galaxies could be modified, in particular if the fraction of small-scale structures such as clusters of galaxies is important (Webster 1985). Therefore, two different effects produced by the cosmological distribution of structures in the universe are expected: a change of the galaxy number count correlated with the mass distribution, namely a magnification bias; and a change of the ellipticity distribution, namely a shear pattern, correlated with the mass distribution as well. Because the expectation values strongly depend on the fraction of non-linear systems and the redshift distribution of the galaxies, it is clear that the analysis of weak lensing effects by large-scale structures is an interesting test of cosmological scenarios.

4.1 Theoretical Expectations

The theoretical investigations of the effect of the large-scale mass distribution on the distribution of ellipticity/orientation of distant galaxies are somewhat simplified by the low density contrast of structures. Beyond 10 Mpc scales, $\delta\rho/\rho \approx 1$ and linear perturbation theory can be applied. On these scales, lenses are no longer considered individually but they are now viewed as a random population which has a cumulative lensing effect on the distant sources. Blandford (1990), Blandford et al (1991) and Miralda-Escudé (1991) first investigated the statistical distribution of distortions induced by large-scale structures in an EdS universe. They computed the two-point polarization (or shear) correlation function and established how the rms value of the polarization depends on the power spectrum of density fluctuations. Kaiser (1992) extended these works and showed how the angular power spectrum of the distortion is related to the three-dimension mass density power spectrum, without assumptions on the nature of fluctuation. These works were generalized later to any arbitrary value of Ω by Villumsen (1996) and Bar-Kana (1996). All these studies concluded that the expected rms amplitude of the distortion is of about one percent, with a typical correlation length of a degree. Therefore it should be measurable with present-day telescopes.

These promising predictions convinced many groups to start investigating more thoroughly how weak lensing maps obtained from wide field imaging surveys could constrain cosmological scenarios. To go into further detail, it is necessary to generalize the previous works to any cosmology and to describe in detail observables and physical quantities that could be valuable to the constraint of cosmological models. Indeed, the investigations of weak lensing by large-scale structures require theoretical and statistical tools that are not different from those currently used for catalogues of galaxies or cosmological microwave background (CMB)-maps. In this respect, the perturbation theory, which has already been demonstrated to work, describes the properties of large-scale structures very well (see Bouchet 1996 and references therein), and seems to be an ideal approach for such large scales. In addition, the use of similar statistical estimators for catalogues of galaxies seems perfectly suited. Bernardeau et al (1997) used the perturbation theory to explore the sensitivity of the second and third moments of the gravitational convergence κ (rather than the distortion whose third moment should be zero), to cosmological scenarios, and to cosmological parameters, including λ-universes. The small angle deviation approximation implies that the distortion of the ray bundle can be computed on the unperturbed geodesic (Born approximation). In the linear regime, if lens-coupling is neglected (see Section 4.4.3), the cumulative effect of structures along the line of sight generates a convergence in the direction $\boldsymbol{\theta}$,

$$\kappa(\boldsymbol{\theta}) = \frac{3}{2}\Omega_0 \int_0^{z_s} n(z_s)\, dz_s \int_0^{\chi(s)} \frac{D_0(z, z_s) D_0(z)}{D_0(z_s)} \delta(\chi, \boldsymbol{\theta})\, (1+z(\chi))\, d\chi, \quad (29)$$

where χ is the radial distance, D_0 is the angular diameter distance, $n(z_s)$ is the redshift distribution of the sources, and

$$\delta = \int \delta_k D_+(z) e^{i\mathbf{k}.\mathbf{x}}\, d^3k \quad (30)$$

is the mass density contrast, which depends on the evolution of the growing modes with redshift, $D_+(z)$. It is related to the power spectrum as usual: $\langle \delta_{\mathbf{k}} \delta_{\mathbf{k}'} \rangle = P(k)\delta_{Dirac}(\mathbf{k}+\mathbf{k}')$. It is worth noting that κ depends explicitly on Ω_0 and not only δ because the amplitude of the convergence depends on the projected mass, not only on the projected mass density contrast.

The dependence of the angular power spectrum of the distortion as a function of (Ω, λ), of the power spectrum of density fluctuations and of the redshift of sources has been investigated in detail in the linear regime by Bernardeau et al (1997) and Kaiser (1998). Bernardeau et al (1997) and Nakamura (1997) computed also the dependence of the skewness of the convergence on cosmological parameters, arguing that it is the first moment which directly probes non-linear structures. From perturbation theory and assuming Gaussian fluctuations, the variance, $\langle \kappa(\boldsymbol{\theta})^2 \rangle$, and the skewness, $s_3 = \langle \kappa(\boldsymbol{\theta})^3 \rangle / \langle \kappa(\boldsymbol{\theta})^2 \rangle^2$, have the following dependencies with the

cosmological quantities:

$$\langle\kappa(\theta)^2\rangle^{1/2} \approx 10^{-2}\,\sigma_8\,\Omega_0^{0.75}\,z_s^{0.8}\left(\frac{\theta}{1^\circ}\right)^{-(n+2)/2}, \tag{31}$$

and

$$s_3(\theta) \approx -42\,\Omega_0^{-0.8}\,z_s^{-1.35}, \tag{32}$$

for a fixed source redshift z_s, where n is the spectral index of the power spectrum of density fluctuations and σ_8 is the normalization of the power spectrum (the rms mass density fluctuation within a sphere of $8h_{100}^{-1}$ Mpc). Hence, since the skewness does not depend on σ_8, the amplitude of fluctuations and Ω_0 can be recovered independently using $\langle\kappa(\theta)^2\rangle$ and s_3. The slope of the projected power spectrum can, in principle, be recovered from the complete reconstruction of the projected mass density, using weak-lensing inversion as discussed in Section 3.

Jain & Seljak (1997), generalizing the early work by Miralda-Escudé (1991), have analyzed the effects of non-linear evolution on $\langle\kappa(\theta)^2\rangle$ and s_3 using the fully non-linear evolution of the power spectrum (Peacock & Dodds 1996). They found formal relations similar to those found by Bernardeau et al. However, on a scale below 10 arcminutes, $\langle\kappa(\theta)^2\rangle$ increases more steeply than the theoretical expectations of the linear theory and is 2 or 3 times higher on scales below 10 arcminutes. These predictions are strengthened by numerical simulations (Jain et al 1998). Therefore, a shear amplitude of about 2–5% is predicted on these scales which should be observed easily with ground-based telescopes (Figure 6). Schneider et al (1998a) recently claimed that they have detected this small-scale *cosmic-shear* signal.

The previous studies are based on the measurements of ellipticities of individual galaxies in order to recover the stretching produced by linear and non-linear structures. Like the mass reconstruction of clusters, it demands high-quality images and an accurate correction of systematics down to a percent level. An alternative to this strategy has been investigated by Villumsen (1996) who looked at the effect of the magnification bias on the two-point galaxy correlation function. Because the magnification may change the galaxy number density as a function of the slope of the galaxy number counts, it similarly modifies the apparent clustering of the galaxies. From Equations 23 and 25, the two-point correlation function averaged over the directions θ is changed by the magnification of the sources and, in the weak lensing regime, its contribution writes (Kaiser 1992, Villumsen 1996, Moessner & Jain 1998):

$$\omega(\theta) = \frac{\langle[N_0(m)(5\alpha-2)\kappa(\theta+\theta')][N_0(m)(5\alpha-2)\kappa(\theta)]\rangle}{N_0(m)^2}, \tag{33}$$

that is,

$$\omega(\theta) = (5\alpha-2)^2\langle\kappa(\theta+\theta')\kappa(\theta)\rangle. \tag{34}$$

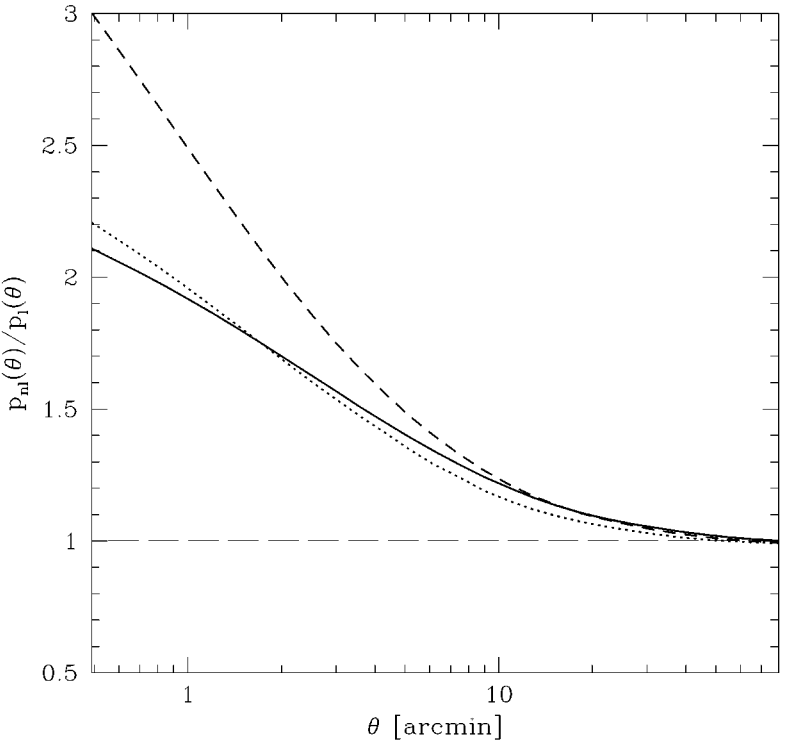

Figure 6 Ratio of the amplitude of the polarization predicted by the non-linear and linear evolution of the power spectrum as a function of angular scale (from Jain & Seljak 1997). The normalization is $\sigma_8 = 1$. The plot shows the expectations for three cosmologies: $\Omega = 1$ (*solid line*), $\Omega = 0.3$ (*dashed line*) and $\Omega = 0.3$, $\lambda = 0.7$ (*dotted line*). The difference between the two regimes becomes significant below the $10'$ scale.

The galaxy two-point correlation function is therefore sensitive to the correlation function of the convergence and to the slope of galaxy counts. If the unlensed two-point correlation function is known, it is then possible to compute the local correlation function of the convergence from the local two-point correlation function of the galaxies.

Detailed investigations of the capability of this technique have been discussed by Moessner et al (1998) who looked at the effect of non-linear clustering on small scales and for different cosmologies. They raised the point that the correlation function can be also affected by the evolution of galaxies which also modifies the two-point correlation function of galaxies, but in an unknown way. Moessner & Jain (1998) proposed a way to disentangle these two effects by using the cross-correlation of two galaxy samples having different redshift distributions that do

not overlap. This minimizes the effect of intrinsic galaxy clustering, but it requires the knowledge of the biasing which can also depend on the redshift. Therefore, the magnification bias method needs auxiliary input that can constrain the biasing independently.

4.2 Measuring the Biasing

Because gravitational lensing is directly sensitive to the total mass responsible for the deflection, it provides a potentially important tool for measuring the biasing factor, as it has been demonstrated by the recent weak lensing analysis of the supercluster MS0302+17 (Kaiser et al 1998). In particular, a well-known effect of the magnification bias is the generation of correlations between foreground and background luminous systems observed in catalogues. The matter associated with the foreground systems can amplify the flux received from background objects, which results in an apparent correlation between the number density or the luminosity of backgound objects and the number density of foregrounds (Canizares 1981). The correlation has been first detected by Fugmann (1990) and confirmed later by Bartelmann & Schneider (1993a,b; 1994) who found correlations of the galaxy number density with the radio-sources of the 1-Jy catalogues, the IRAS catalog, and the X-ray galaxies. Further independent analyses of such associations showed also evidences of magnification bias (Bartelmann et al 1994, Rodrigues-Williams & Hogan 1994, Seitz & Schneider 1995b, Wu & Han 1995, Benítez & Martínez-González 1997, Williams & Irwin 1998). The statistical basis of these associations is surprisingly robust and difficult to explain physically without invoking lensing effects.

Bartelmann et al (1994) argued that the correlation can be interpreted has a magnification bias only if it is produced by condensations of matter, like clusters of galaxies (Bartelmann & Schneider 1993a). In order to check this hypothesis, Fort et al (1996) have attempted to detect weak shear around some selected bright quasars which could be good lensing candidates. They found strong evidence of weak shear around half of their sample with, in addition, a clear detection of galaxy overdensities in the neighborhood of each quasar. The Fort et al sample has been re-analyzed recently by Schneider et al (1998a) and the detection has been strengthened on a more reliable statistical basis, with a firm confirmation for one of the quasars from the HST images obtained by Bower & Smail (1997). In addition, some other observations have also detected gravitational shear around bright radiosources: Bonnet et al (1993) found a shear signal around the double imaged quasar Q2345+007, which was later confirmed to be associated with a distant cluster (Mellier et al 1994; Fischer et al 1994; Pelléo et al 1996). Similar detection of a cluster has recently been reported around the Cloverleaf (Kneib et al 1998) and around 3C324, which also clearly shows a shear pattern from the HST images (Smail & Dickinson 1995). The sample is nevertheless too small to provide a significant direct evidence that magnification bias is detected in quasar catalogues. Indeed, it would be important to pursue this program using a large

sample of bright quasars or radiosources. The field of view does need to be large, so the HST with the Advanced Camera could be a perfect instrument for this project. The impact of such magnification bias could be important for our understanding of the evolution scheme of quasars and galaxies, because it changes the apparent luminosity functions of these samples (Schneider 1992, Zhu & Wu 1997).

If these correlations are caused by magnification bias, a quantitative value of the biasing can in principle be estimated, for instance from the angular foreground-background correlation function (Kaiser 1992), where foreground could be galaxies or dark matter. Bartelmann (1995a) expressed the angular quasar-galaxy correlation, ξ_{QG}, as a function of the biasing factor, b, and the magnification-mass density contrast cross-correlation function, $\xi_{\mu\delta}$, in the weak lensing regime:

$$\xi_{QG}(\boldsymbol{\theta}) = (2.5\alpha - 1)\, b\, \xi_{\mu\delta}(\boldsymbol{\theta}), \tag{35}$$

where α is the slope of the background galaxy counts. However, since $\xi_{\mu\delta}$ depends on the power spectrum of the projected mass density contrast, the determination of the biasing factor is possible only if one independently obtains the amplitude of the power spectrum. Generalizations to non-linear evolution of the power spectrum and to any cosmology were explored by Dolag & Bartelmann (1997) and Sanz et al (1997). As expected, the non-linear condensations increase the correlation on small scales by a very large amount; that, however, still strongly depends on the amplitude of the power spectrum.

With the observation of weak lensing induced by large-scale structures, it becomes possible to observe directly the correlation between the background galaxies and the projected mass density of foreground structures instead of using the light distribution emitted by the foreground galaxies. Following the earlier development by Kaiser (1992), Schneider (1998) has computed the cross-correlation between the projected mass, M, and the galaxy number density of foreground galaxies, N, on a given scale θ, $\langle MN\rangle_\theta$, as a function of the biasing factor of the foreground structures, b. Like previous studies, it is simply proportional to b, but it also depends on σ_8 and the slope of the power spectrum, and as such it is not trivial to estimate it without ambiguity. A more detailed investigation of the interest of $\langle MN\rangle_\theta$ has been done by Van Waerbeke (1998a) who computed the ratio, $R(\theta)$ of the density-shear correlation over the two-point galaxy correlation function for a narrow redshift distribution of foregrounds and a narrow range in scale (Van Waerbeke 1998a,b):

$$R_\theta = \frac{3}{2}\frac{\Omega}{b}\frac{g(w_f)\, f_K(w_f) N_f(w_f)}{a(w_f)\ \int N_f^2(w)\, dw}, \tag{36}$$

where a is the expansion factor, w_f is the comoving distance of the foreground, f_K is the comoving angular diameter distance, N_f is the redshift distribution of the foreground galaxies, and

$$g(w) = \int_w^{w_f} N_b(w') \frac{f_K(w' - w)}{f_K(w')}, \tag{37}$$

$N_b(w')$ being the redshift distribution of the background galaxies. Using this ratio, he investigated the scale dependence of the biasing, including the non-linear spectrum and different cosmologies, and discussed how it can be used to analyze the evolution of the biasing with redshift, if two different populations of foregrounds are observed. The ratio $R_\theta / R_{\theta'}$ permits one to compare the biasing on two different scales. This quantity does not depend on Ω, on the power spectrum or on the smoothing scale, so it is a direct estimate of the evolution of biasing with scale. Van Waerbeke predicts that a variation of 20% of the bias on scales between $1'$ and $10'$ will be detectable on a survey covering 25 square degrees. This ratio is therefore a promising estimator of the scale dependence of the biasing.

The analysis discussed above indicates the potential interest of lensing to the study of the evolution of bias with scale and redshift of foreground, with the direct use of the correlation between the ellipticity distribution of background sources and the projected mass density inferred from mass reconstruction. It thus permits an accurate and direct study of the biasing and its evolution with look-back time and possibly with scale. However, it is worth stressing that Van Waerbeke (like Bartelmann 1995a and others) assumed a linear biasing. In the future it will be important to explore in detail the generalization to a non-linear bias (Van Waerbeke, private communication) as described by Dekel & Lahav (1998).

4.3 Strategies for Weak Lensing Surveys

The rather optimistic predictions from theoretical work reported in Section 4.1 are convincing enough to investigate in great detail how weak lensing surveys can be designed in order to maximize the signal to noise ratio of statistical and physical quantities, as well as to minimize the time spent for the survey. The definition of a best strategy addresses many issues: size, shape, topology of the survey, best statistical estimators, optimal analysis of the catalogues and best extraction of the signal from the raw data. This last point (measurement of ellipticities, correction of the PSF) has already been discussed in Section 3.3, so I will focus on the other aspects. Indeed, weak lensing surveys have rather generic constraints which are common to any survey in cosmology (see Szapudi & Colombi 1996, Kaiser 1998, Colombi et al 1998 and references therein). The main sources of noise are the cosmic variance, the intrinsic ellipticity distribution of the lensed galaxies and possibly the noise propagation during the mass reconstruction from lensing inversion. In addition, at such low shear level, the correction of the PSF, as well as the removals of systematics coming from optical and atmospheric degradation of the images, or from the method used to measure the shear from galaxy ellipticity, are crucial steps.

The impact of the size, the shape and the deepness of weak lensing surveys has been addressed by Blandford et al (1991) and Kaiser (1992) and has been investigated in more detail by Kaiser (1998), Kamionkowski et al (1998), Van Waerbeke et al (1999), and Jain et al (1998). Depending on the scientific goals

and the nature of the data, medium-size deep, very-wide shallow and very-small ultra-deep surveys have been proposed.

The most detailed investigation done so far has been conducted by Van Waerbeke et al (1999). From a sample of 60 simulations per set of parameters they computed the expected signal to noise ratio of the variance and the skewness of the convergence, and they attempted to reconstruct the projected mass density from the lensing signal in order to recover the projected power spectrum for each model on $5^\circ \times 5^\circ$ and $10^\circ \times 10^\circ$ noisy maps. They included various cosmologies, mass density power spectra, sampling strategies and redshifts of sources. This work is a preparation of the subarcsecond seeing survey which should be conducted at CFHT with the new wide field Megacam camera (which will cover one square degree, Boulade et al 1998). These simulations show that the projected mass density maps can be recovered with an impressive accuracy and demonstrate that such a survey will be able to recover the projected power spectrum of mass density fluctuations, from 2.5 arcminutes up to 2 degrees with a signal to noise ranging from 10 to 3. The power spectrum on small scales is dominated by the shot noise due to the intrinsic ellipticity distribution of the background galaxies, but it follows the statistics predicted by Kaiser (1998) which permits its easy removal. The best strategy suggested by these simulations is a shallow survey with a typical galaxy number density of 30 arcmin^{-2} over 10×10 square degrees. According to Van Waerbeke et al (1999) it will permit one to separate $\Omega = 0.3$ from $\Omega = 1$ universes at a 6σ confidence level Figure 7). Kaiser (1998) recommends a wide field as well, but suggests a sparse sampling on a very large scale rather than a compact topology. This alternative has not been investigated yet using simulations. In particular, it would be useful to have quantitative estimates of the scale beyond which the survey should switch from a compact to a sparse sampling of the sky.

Alternatively, Stebbins (1996) and Kamionkowski et al (1998) have explored the possibility of using shallower surveys, which sample the sky with only a few galaxies per arcminute, but cover about half the sky. Contrary to the Megacam-like surveys which aim at mapping the shear field and building a map of the projected mass density, these shallow surveys only aim at measuring the correlation of ellipticities on very large scales. Stebbins (1996, 1999) used the linear theory to compute the angular power spectrum of the shear inferred from a tensor spherical harmonic expansion of the shear pattern of an all-sky survey. He argues that the SDSS could provide reliable information on the projected angular power spectrum of the shear. The expected signal is very small, because most of the galaxies will be at a redshift lower than 0.2. The seeing of the site and the sampling of the images could have minor impact on the signal because these nearby galaxies should be much larger than the seeing disk. However, a simulation of the systematics which include the quality of the telescope and the instruments, as well as an estimate of the possible systematics produced by the drift-scanning are now necessary in order to have a clear quantitative estimate of the expected signal to noise ratio.

The use of the VLA-FIRST radio survey for weak lensing proposed by Kamionkowski et al (1998) looks promising. FIRST covers about the same area

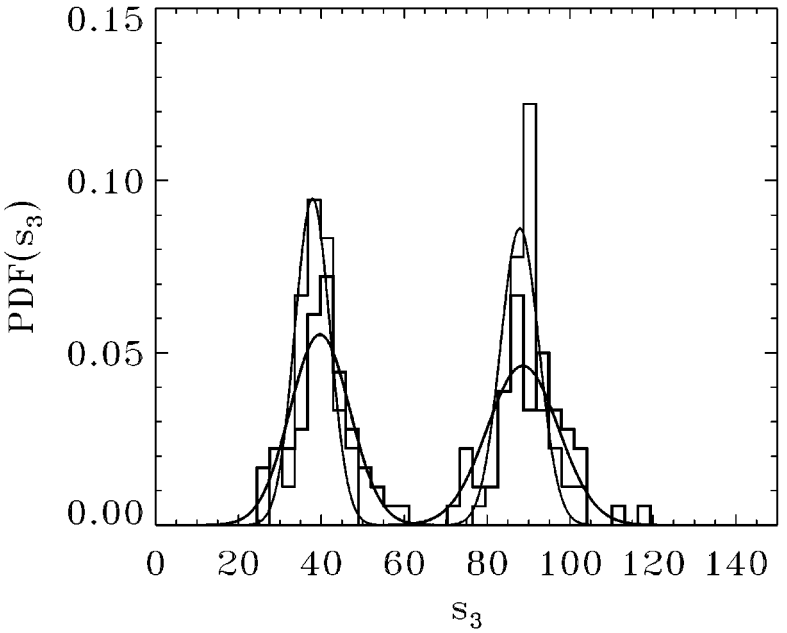

Figure 7 Histograms of the values of the skewness of the convergence for an $\Omega = 1$ (*right*) and $\Omega = 0.3$ (*left*) universe and for a 5×5 (*thick lines*) and 10×10 (*thin lines*) square degrees survey. This simulates the possible surveys to be done with MEGACAM at CFHT (from Van Waerbeke et al 1998).

as the SDSS but the radiosource sample has a much broader redshift distribution and a median redshift beyond $z = 0.2$. However, with less than 100 sources per square degree, the sampling is rather poor. Kamionkowski et al predict an rms ellipticity of about 3% on 6 arcminutes, 1% on 20 arcminutes and on one degree scale, with a signal to noise ratio larger than 5, in good agreement with Bernardeau et al (1997) and Jain & Seljak (1997). Preliminary results from this survey should soon be available.

On small scales, first attempts for measuring cosmic shear have already been made by several groups. Mould et al (1994) used a very deep image obtained at the Palomar Telescope to measure cosmic shear on a scale of 5 arcminutes. They do not find a significant signal (however, see JV Villumsen 1995, unpublished results) and argued that the cosmological signal of their field is below 4%. A similar attempt has been made by Fahlman et al (1994) on a 15 arcmin field. The images were obtained at CFHT in subarcsecond seeing conditions ($\approx 0.5''$, against $0.9''$ for Mould et al), but significantly less deep than the Mould et al observations. Fahlman et al did not detect any significant signal, though owing to the excellent seeing, they expected it to be three times more sensitive. On the other hand, a weak lensing signal has already been detected on a 2 arcmin

scale around radiosources and quasars (see Section 4.2), which shows that cosmic shear on a small scale is detectable. Schneider et al (1998a) argued that the shear detected around radiosources is cosmic shear, though the sample is probably biased toward non-linear structures because the fields are preferentially selected around bright quasars. This is probable because the motivation of the Fort et al (1996) observations (from which the Fort et al and Schneider et al sample is based) was the verification of the Bartelmann et al (1994) hypothesis that the quasar-galaxy association results from a magnification bias of bright quasar samples by large-scale structures. Therefore, if the magnification bias really works then the cosmological significance of the Schneider et al (1998a) interpretation is difficult to quantify. Conversely, if the quasar-galaxy associations are not produced by such magnification, then Schneider et al measured the cosmic shear for the first time.

Several low-angular scale surveys are under way to provide significantly better statistics. These surveys have been summarized by Seitz et al (1999). A promising strategy consists of using the parallel Space Telescope Imaging Spectrometer (STIS) observations of HST as randomly selected fields. For each of those outstanding images, it is possible to measure the average distortion with a very high confidence level. Preliminary analyses by Seitz et al (1999) show that the PSF is incredibly stable and that the first observations lead to an rms ellipticity of 3% on one arcminute scale, which is very encouraging. However, for the moment it is difficult to interpret the rms shear in terms of constraints for cosmological models because the STIS parallel observations are done without filter, so there is no color information on the lensed galaxies to constrain their average redshift.

In addition to the definition of the survey strategy, the scientific return is sensitive to the technique used to analyze the catalogues. In this respect, the best procedure depends on the noise properties on the survey. In theory, if the noise follows Gaussian statistics, the Wiener filtering should provide a minimum variance estimator of cosmological quantities (Seljak 1997a). However, it is not obvious that this is the best approach, in particular on small scales where non-linear features deviate significantly from gaussianity. For instance, Kruse & Schneider (1999) have explored a strategy for an optimal extraction of the high density peaks present in surveys. It uses the aperture mass densitometry for cosmic shear measurement proposed by Schneider et al (1998b) which permits the detection of peaks of the projected mass density as function of the tangential shear, γ_t (Kaiser 1995). This simple and rather robust approach which focuses on the most contrasted systems should provide in a simple way some constraints of the number density of high peaks, and therefore of the cosmological scenarios. Schneider et al (1998b) argued that the use of a compensated filter is an optimal procedure to measure κ from γ without mass reconstruction because in contrast to the top hat filter, it selects a sharp scale range that cancels the additional noise produced by the adjacent wave numbers. The merit of the two filterings has also been investigated in detail in the simulations of Van Waerbeke et al (1999). They found that the best choice is unclear: the compensated filter is better for the variance, but is worse for the skewness (see Figure 8, color).

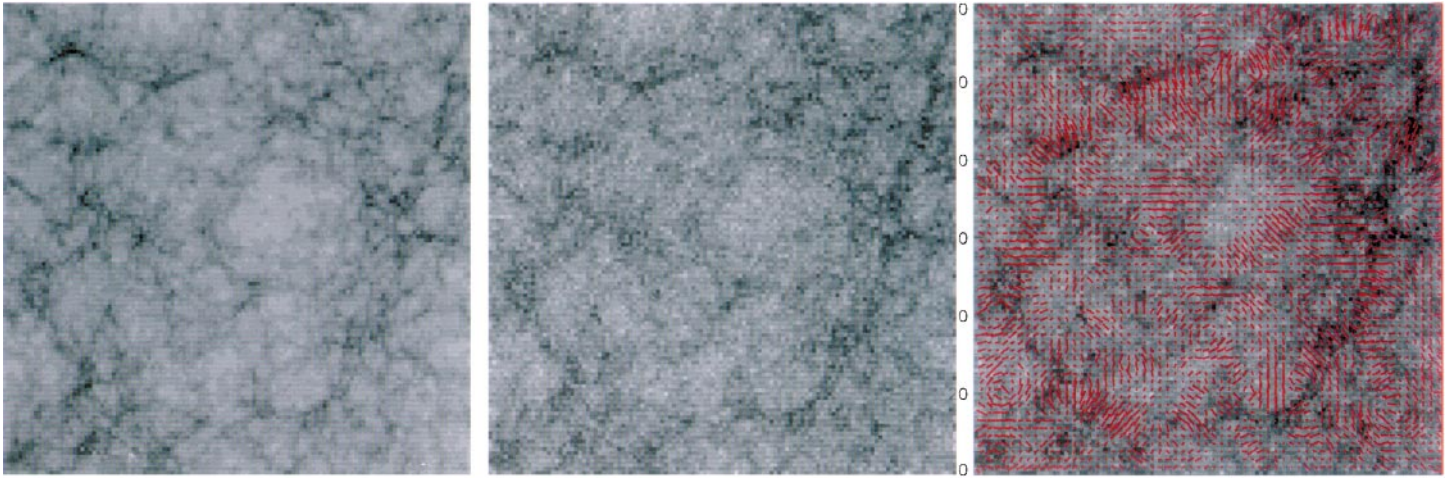

Figure 8 Simulation of mass maps construction from a wide field weak lensing survey. The left panel is the original simulated projected mass density of large scale structures. The field covers 25 square degrees. The middle panel is the reconstructed mass map using the algorithm described in Van Waerbeke et al (1998). The noise introduced in the simulated map is due to the intrinsic ellipticity distribution of the lensed galaxies. The similarity with the original mass map is striking. The right panel is the shear map overlayed to the projected mass map. The length and the orientation of each line indicate the amplitude and the orientation of the shear.

4.4 Critical Issues

The critical issues already discussed for the weak lensing and mass reconstruction of clusters of galaxies are valid and even more critical for large-scale structures. This will not be discussed again here, but we should mention that systematic effects are a real concern which could be an ultimate limitation of the weak lensing capabilities, at least on ground-based telescopes.

Redshift of Sources Equations 27 and 28 show a strong dependence of the variance and the skewness of the convergence on the redshift distribution of the lensed sources. As far as weak lensing is concerned, from the investigations of the effect of redshift distribution of sources on cluster mass reconstruction, it seems that only the averaged redshift of the galaxies and the width of their distribution are needed (Seitz & Schneider 1997), even with a bad precision (say, $\Delta z_s \approx 0.5$). This requirement is therefore not severe and can be obtained using photometric redshifts. The work by Connolly et al (1995) demonstrates that galaxies brighter than $I = 22.5$ can easily be calibrated using spectroscopic redshifts and that photometric information in 4 different filters constrain the redshift of these galaxies with an accuracy of about $\Delta z_s \approx 0.05$. The future surveys with 10-meter class telescopes will calibrate photometric redshift up to $I = 23.5$ and even fainter, by using Lyman-break galaxies (Steidel et al 1998) and near-infrared photometry. This is deep enough for shallow wide field surveys so one can be reasonably confident that the redshift distribution of the lensed galaxies will not be a major problem. Conversely, this is another argument in favor of shallow rather than deep surveys which would reach limiting magnitudes beyond the capabilities of spectrographs. Indeed, as shown by Van Waerbeke et al (1999) the signal to noise ratio of the variance and the skewness does not strongly depend on the redshift of the sources, so it is useless to reach very faint magnitudes.

Source Clustering Due to the intrinsic clustering of the galaxies, the redshift distribution can be broad enough to mix together the population of lensed galaxies and the galaxies associated with the lensing structures. In particular, an extended massive structure at high redshift can play simultaneously the role of a lens and a reservoir of lensed galaxies. The average redshift distribution of the sources can therefore be biased by the galaxies located within the massive structure, which can bias as well the estimated value of the convergence in a similar way. Indeed, the variance of the convergence is not affected by this clustering (Bernardeau 1998a). However, the skewness is much more affected, mainly because the overlapping acts exactly as a non-linear evolution of the projected density. Bernardeau (1998a) shows that most of these effects are negligible on scales beyond 10 arcminutes. It would also be interesting to investigate more deeply how the source clustering may contribute to spurious signals on small scales.

The apparent change of the two-point correlation function by magnification bias can also change the local redshift distribution of lensed sources. This effect, though mentioned by Bernardeau (1998a), has not been investigated in detail.

Lens Coupling When ray bundles cross two lenses by accident, the cumulative convergence is given by the product of the magnification matrix, and not simply the sum of the two convergences. The resulting convergence contains additional coupling terms that must be estimated. Fortunately, in the weak lensing regime, this coupling appears to be negligible. It does not change the value of the variance, and the skewness is only weakly modified (Bernardeau et al 1997, Schneider et al 1997).

Validity of the Born Approximation The effects of mass density fluctuations caused by large-scale structures on the deformation of the ray bundles are computed assuming that the Born approximation is valid, that is, the deformation can be computed along the unperturbed geodesic. In the case of linear perturbations, this assumption is valid at the lowest order. As discussed by Bernardeau et al (1997), the correction on the skewness should be at the percent level. However, this is less obvious once lens couplings are taken into account. The validity of the Born approximation has not been tested in detail, so far. This certainly deserves inspection using high-resolution numerical simulations. The simulations done by Jain & al (1998) or Wambsganss et al (1998) could provide valuable information on this issue.

Intrinsic Correlated Polarization of Galaxies It is possible that the intrinsic orientations of galaxies are not randomly distributed but have a coherent alignment correlated to the geometry of the large-scale structures in which they are embedded (Bingelli 1982). If so, the coherent alignment produced by weak lensing will be contaminated by the intrinsic alignment of the galaxies, and a mass reconstruction based on the shear pattern will be impossible. Such alignments could appear during the formation of large-scale structures or could result from dynamical evolution of galaxies within deep potential wells, such as superclusters or clusters of galaxies (see Coutts 1996, Garrido et al 1993 and references therein). However, the most recent numerical simulations do not show such correlations. Many attempts have been made to search for signatures of these intrinsic coherent patterns. So far, no convincing observations of nearby structures have demonstrated that there are large-scale coherent alignments. This possibility has to be investigated thoroughly, in particular in nearby large-scale structures where a coherent alignment from gravitational lensing effect is negligible. It would be valuable to have more quantitative estimates of possible trends for alignments from future very high-resolution numerical simulations of structure formation.

5. GALAXY-GALAXY LENSING IN FIELD GALAXIES

Evidence that galaxies have dark halos comes from the kinematical and dynamical studies of galaxies. However, the geometry of the halos and the amount and distribution of dark matter are unknown and in practice difficult to probe. Gravitational lensing could provide valuable insight in this field: because it works on

all scales, in principle the halos of galactic dark matter should be observed from their gravitational lensing effects on background galaxies. The first Einstein rings and the other galaxy-scale lensing candidates have provided unique opportunities to measure the mass-to-light ratios and to probe the mass profiles of a few galaxies (Kochanek 1991). In the case of rings, the mass of the lensing galaxies can be very well constrained (see, for instance, Kochanek 1995), so the properties of the halos inferred from modeling are reliable. However, Einstein rings are rare lensing events, so the sample is still very small.

A more promising approach consists of a statistical study of the deformation of distant galaxies by foreground galactic halos. The galaxy-galaxy lensing analysis uses the correlation between the position of foreground galaxies and the position-alignment of their angular-nearest neighbors among the background population. If the alignment is assumed to be produced by the gravitational shear of the foreground halos, then it is possible to probe the mass of the halos, if the redshift distributions of the foregrounds and the backgrounds are known. A statistical analysis is then possible, if one assumes that all the foreground galaxies have similar halos, which can be scaled using the Tully-Fisher relation and the photometric data (galaxy luminosity). The expected gravitational distortion is very weak: for foregrounds at redshift $\langle z_l \rangle = 0.1$, backgrounds at $\langle z_s \rangle = 0.5$, and typical halos with velocity dispersion of 200 kms^{-1} and radius of 100 kpc, $|\gamma| \approx 1\%$ at about 20 kpc from the center. But if the observations go to very faint magnitudes there is a huge number of background lensed galaxies, so that the weakness of the signal is compensated by the large statistics. It is worth pointing out that the signal-to-noise ratio depends on the number of galaxy pairs, so either very wide field shallow surveys or ultra-deep imaging can be used for the statistics (although they will not probe similar angular scales).

Tyson et al (1984) made the first attempt, using approximately 50,000 background and 11,000 foreground galaxies obtained from photographic plates. The 3σ upper limit of the circular velocity that they found was 160 km.sec^{-1}, with a maximum cutoff radius below $50h_{100}^{-1}$ kpc. These values are significantly smaller than theoretical expectations from rotation curves and dynamical analyses of galaxies. However, despite a careful examination of possible systematics (Tyson et al 1984, Tyson 1985), there are two limitations to Tyson et al's pioneering work. First, as emphasized by Kovner & Milgrom (1987), the assumption that background galaxies are at infinite distances has considerable impact on the constraints on the circular velocity and the cutoff radius. If one includes a corrective factor which takes into account the distances of the sources, the upper limit for the circular velocity is considerably higher (330 kms^{-1} for a L_* galaxy) and no constraints can be put on the cutoff radius (Kovner & Milgrom 1987). Second, the image quality of the photographic plate is poor and may also affect the measurement of weak distortions.

The first attempt to use deep CCD subarcsecond images was made by Brainerd et al (1996) using about 5,000 galaxies. The distortion was compared with simulations, based on analytical profiles for the dark matter halos, and the Tully-Fisher

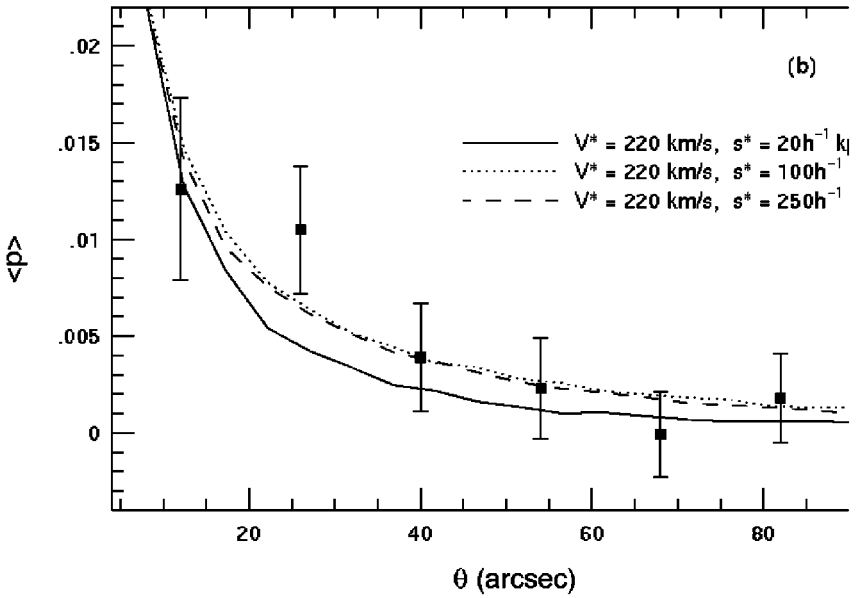

Figure 9 Angular variation of polarization produced by weak lensing of foreground galaxies on the background (lensed) sources in the Brainerd et al (1996) sample. The lines show theoretical expectations for three models of halos having different velocity dispersion and scales.

relation, in order to relate mass models to observations. After careful investigations of systematics, they detected a significant polarization of about 1%, averaged over a separation between $5''$ and $34''$ (see Figure 9). They concluded that halos smaller than $10h^{-1}$ kpc are excluded at a 2σ level, but the data are compatible with halos larger than $100h^{-1}$ kpc and circular velocities of 200 kms^{-1}. Similar works using 23,000 galaxies have been done recently using very deep images obtained with MOCAM at CFHT (Cuillandre et al 1996) with seeing below $0.7''$. They found remarkably similar results as Brainerd et al for the polarization and its evolution with radius (Erben et al, in preparation).

The HST data look perfectly suited for this kind of program which demands high image quality and the observation of many field galaxies. Griffiths et al (1996) used the Medium Deep Survey (MDS) and measured the distortion produced by foreground elliptical and spiral galaxies. They found results similar to those of Brainerd et al (1996) but with a signal more significant for foreground elliptical than spiral galaxies. The comparison with shear signals expected from various analytical models seems to rule out de Vaucouleurs' law as mass density profile of ellipticals. Ebbels et al (in preparation) are now extending the MDS work to a larger sample, trying to simulate more carefully the selection effects. Dell'Antonio & Tyson (1996) and Hudson et al (1998) analyzed the galaxy-galaxy lensing signal in

the HDF. As compared with the ground-based images or the MDS, the field is small but the depth permits the use of many background galaxies even on a scale smaller than 5 arcseconds. Furthermore, the UBRI data of the HDF permit the inference of accurate photometric redshifts for the complete sample of galaxies. Dell'Antonio & Tyson compared the lensing signal with predictions from an analytical model for the halo. They found a significant distortion of about 7% at $2''$ from the halo center which corresponds to halos with typical circular velocities of less than 200 km.sec^{-1}. The results obtained by Hudson et al (1998) are consistent with those of Dell'Antonio & Tyson (1996) and Brainerd et al (1996). However, their maximum-likelihood analysis more accurately takes into account the collective effects of large-sized halos (Schneider & Rix 1997). In contrast to previous studies, Hudson et al made careful corrections of images from the PSF and scaled the magnitude inferred from the analytical models of the halos using the Tully-Fischer relation.

Galaxy-galaxy lensing is potentially a very valuable tool for studying the dynamics of galaxies, complementary of standard methods using photometry and spectroscopic data. Because the foreground galaxies have an average redshift of approximately 0.1, galaxy-galaxy lensing also offers an opportunity to look at the dynamical evolution of galaxies by comparing local galaxies at redshift zero to intermediate-redshift galaxies (Hudson et al 1998). However, there are still some limitations due to the rather small number of galaxies used in each sample. As shown from the simulations by Schneider & Rix, it is rather easy to constrain the velocity dispersion of the halos, but more difficult to put limits on their physical scale (see Figure 10). There are also uncertainties coming from the models of halos (which are assumed to be spherical) and the additional noise produced by cosmic shear which can contaminate the galaxy-galaxy signal. Although these issues should be analyzed in more detail in the future, dramatic changes in the results are not expected (Schneider & Rix 1997). In particular, the weak lensing induced by large-scale structures should indeed be canceled by the averaging procedure of galaxy-galaxy lensing.

6. GRAVITATIONAL TELESCOPE AND HIGH-Z UNIVERSE

6.1 Redshift Distribution of Galaxies Beyond B = 25

Gravitational lensing magnifies part of the distant universe and permits exploration of the redshift distribution of faint galaxies as well as the morphology and the contents of very distant galaxies. As discussed in Section 4.4, information on the distances of the sources is relevant for the weak lensing inversion, because the mass reconstruction uses a grid of faint distant sources whose redshift distribution is basically unknown. In particular, this hampers the mass estimates of high-redshift lensing clusters which are very sensitive to the redshifts of the background

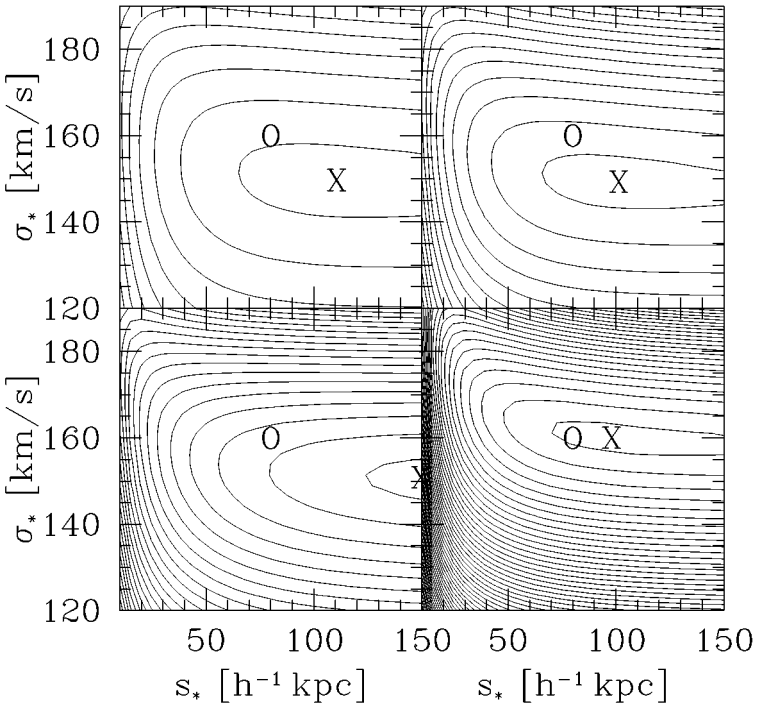

Figure 10 Simulations of galaxy-galaxy lensing done by Schneider & Rix (1997) for four samples of galaxies: 795 (*top left*), 1165 (*top right*), 2169 (*bottom left*) and 3137 (*bottom right*). The O symbol indicates the input parameters of the model and the X shows the maximum of the likelihood function. The likelihood isocontours shows that the velocity dispersion is recovered easily, in contrast to the scale which requires many more galaxies.

sources (Luppino & Kaiser 1997). Unfortunately, beyond $B = 25$, even giant optical telescopes are too small for spectroscopy and the redshift of a complete sample of $B > 25$ galaxies cannot be secured in a reasonable amount of observing time. The possibility of using photometric redshifts is very promising, but observations as well as tests of the reliability of the method for the faintest galaxies are still underway and require careful control. Moreover, because it is hopeless to calibrate the photometric redshifts of the faint samples with spectroscopic data, a cross-check of the predictions of photometric redshift and "lensing-redshift" is important.

Spectroscopic Surveys of Arclets Spectroscopic surveys of redshifts of arc(let)s are long and difficult tasks but are definitely indispensable for lensing studies. They permit computation of the angular distances D_{OL}, D_{LS} and D_{OS} and therefore obtain the absolute scaling of the projected mass density. These redshifts also directly

probe the positions of critical lines which eventually constrain the local mass distribution for some detailed models (Kneib et al 1993, 1996; Natarajan et al 1998; Kneib et al, in preparation). The development of the lensing inversion technique (see Section 6.1.2) also requires spectroscopic confirmations of its predictions to demonstrate that this is a reliable and efficient method. Last but not least, it is in principle also possible to obtain information on the cosmological parameters if one could have enough redshifts to constrain both the mass distribution of the lens and the geometry of the Universe.

Spectroscopic surveys of the "brightest" arclets in many clusters are progressing well. Some extremely distant galaxies have been discovered, such as the arc(let)s in Cl13587+6245 at $z = 4.92$ (Franx et al 1997, see Figure 11), in A1689 at $z = 4.88$ (Frye & Broadhurst, private communication), in A2390 at $z = 4.04$ (Frye & Broadhurst 1998), in Cl0939+4713, where three $z > 3$ arcs have been detected (Trager et al 1997), or the hyperluminous galaxy in A370 at $z = 2.8$ (Ivison et al 1998). Extensive spectroscopic follow-up is also under way in A2390 (Bézecourt & Soucail 1997, Frye et al 1998) and in A2218 (Ebbels et al 1996, 1998). The spectroscopic observation by Frye et al (1998) is a good example of what could be expected from redshifts of arc(let)s: from their Keck observations,

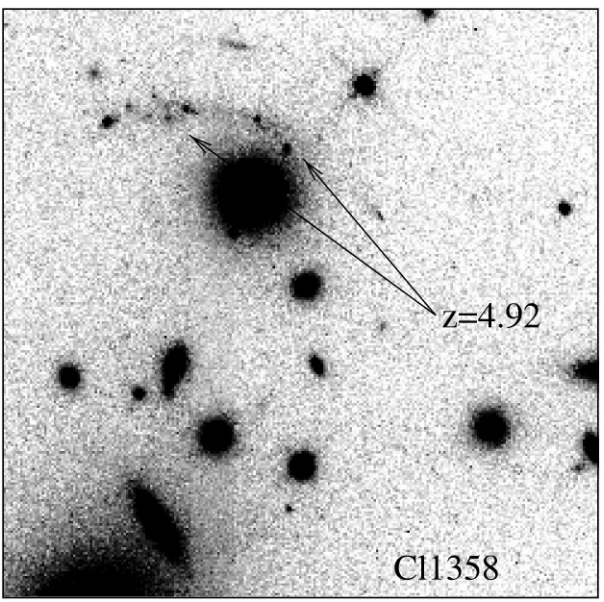

Figure 11 The giant arc detected in Cl1358+6245 is the most distant arc ever observed ($z = 4.92$). The strong magnification permits the detection of some inner structures in a lensed galaxy at $z \approx 5$. Many bright spots are visible (Franx et al 1997). The brightest spot on the left is also visible in the Soifer et al (1998) J-band observations and seems to be a dense core.

they show that the straight arc in A2390 is actually composed of two lensed galaxies aligned along the same direction, one at $z = 0.931$ (reported earlier by Pelló et al 1991) and the other one at $z = 1.033$. These observations confirm the early conclusions from multicolor photometry (Smail et al 1993) as well as from theoretical considerations (Kassiola et al 1992b) that this straight arc should be composed of two galaxies.

About 50 redshifts of arc(let)s have been measured so far. However, from this sample it is difficult to infer valuable information on the redshift distribution of $B > 25$ galaxies or to constrain evolution models of galaxies because it is biased in an unknown way. Since most of these objects are very faint, only arclets showing bright spots on HST images revealing star-forming regions are generally selected. These features, which increase the probability of detecting emission lines, optimize the chance to get reliable redshifts but generate a sample of arclets where star forming galaxies are preferentialy selected. Furthermore, owing to the steep slope of galaxy counts beyond $B = 25$ the magnification bias favors observations of blue galaxies rather than red ones. So, even if the spectroscopy of arclets is crucial for the lens modeling and eventually to obtain the spectral energy distribution of high-redshift galaxies, the spectroscopic sample of arc(let)s must be handled carefully and a detailed analysis of the selection function is needed prior to statistical studies. In the meantime, it is important to focus on getting a few spectra of extremely high-redshift galaxies ($z > 5$) that could be observable thanks to high magnification.

Redshift Distribution from Lensing Inversion If it is possible to recover the lensing potential with good accuracy, the lensing equation can be inverted in order to send the lensed image back to its source plane. The shape of the source can in principle be predicted for any redshift beyond the lens position. The basic principle of the lensing-inversion approach was initially discussed by Kochanek (1990) and refined later by Kneib et al (1994, 1996). If the shape of the galaxies sent back beyond the lens plane is parameterized by the quantity $\tau = (a^2 - b^2)/2ab\, e^{2i\theta}$, then it is easy to show that in the weak lensing regime, the complex quantity $\boldsymbol{\tau}_I$ and its projection on a y-axis, τ_y, writes (Kneib et al 1994, 1996):

$$\boldsymbol{\tau}_I = \boldsymbol{\tau} + \boldsymbol{\tau}_S; \quad \tau_{S_y} = \tau_{I_y}, \tag{38}$$

where the subscripts I and S refer to the image and the source, respectively. Therefore, τ_y is an invariant. The conditional probability of a source to be at redshift z, given the shape and the position of the image, and for a given mass model is:

$$p(z \mid model) = \frac{p(\tau_{S_x}; \tau_{S_y})}{p(\tau_{S_y})}. \tag{39}$$

For a simple distribution of the shape of the sources, it turns out that this probability is maximum at the redshift where the deformation of the source is minimized. Therefore, the lensing-inversion predicts that the most probable redshift, for a given

model, is where the unlensed galaxies have a minimum ellipticity. This intuitive assumption proposed by Kneib et al (1994) was established on an observational basis by Kneib et al (1996) using the HST-MDF galaxies as a fair sample of unlensed sources. The obvious interest of this method is that it does not depend on the magnitude of the arclet but on its position and its shape in the image plane. Potentially, it provides the redshift of any arclet up to the limiting magnitude of the observations.

The lensing inversion was first applied on A370 (Kochanek 1990, Kneib et al 1994), from the lens modeling of the giant arc and some multiple images. Though the (unlensed) magnitude-redshift diagram found for these arclets shows a good continuity with the faint spectroscopic surveys (Mellier 1997), some of the predicted redshifts are uncertain. In fact, as shown by Fort & Mellier (1994, Figure 12), the X-ray isophotes and the arclet positions do not follow the expectations of the lens modeling of the eastern region. This is an indication that although the modeling is excellent in the cluster center, the mass distribution does not have a simple geometry beyond the giant arc and therefore the lens model in this region is uncertain. Similar complex substructures could exist on scales below the resolution of the mass maps and could also produce wrong redshift estimates. Furthermore, the lensing inversion is also sensitive to the accuracy of the shape measurements of each arclet, which in the case of very faint objects could be an important source of uncertainty.

There are two solutions to solve these issues: first, it is highly preferable to use HST images instead of ground based images. The recent spectroscopic confirmations by Ebbels et al (1996, 1998) of most of the redshifts predicted from the lensing-inversion in A2218 from the HST data (Kneib et al 1996) are wonderful demonstrations of the capabilities of such a technique when used with superb images. Second, it is important to focus on lensing-clusters with simple geometry in order to lower the uncertainties on the lens modeling. In this respect, though A370 and A2218 are rather well modeled, they are not the simplest, and clusters such as MS0440, A1689 or MS2137-23 appear to be better candidates.

Probing Source Redshifts Using Various Lens Planes A more natural and simple way to infer the redshift distribution of the faint galaxies is to look for arc(let)s or weak lensing signals through a set of different lensing clusters having increasing redshifts. The ratio of lensed versus unlensed faint galaxies and the amplitude of the shear patterns as a function of redshift directly probe the spatial distribution of the galaxies along the line of sight. This idea was tentatively explored by Smail et al (1994) who analyzed the lensing signal in three lensing clusters at redshifts 0.26, 0.55 and 0.89. They found that most $I < 25$ objects cannot be low-z dwarf galaxies and concluded that a large fraction of $I = 25$ galaxies are beyond $z = 0.55$. The absence of any significant lensing signal in the most distant cluster led to inconclusive results on the fraction of these galaxies that could be at very large redshift. Fortunately, the distant clusters observed by Luppino & Kaiser (1996) and Clowe et al (1998) provided considerable insights about the high-redshift tail of faint galaxies. The detection of weak lensing in three $z > 0.75$ clusters put

strong constraints on their samples of $23.5 < I < 25.5$ galaxies, which must be dominated by a $z > 1$ population. These three lensing clusters strengthen the conclusions obtained from the shear detected around Q2345+007 (Bonnet et al 1993) which is also produced by a high-redshift cluster (Mellier et al 1994, Fischer et al 1994, Pelló et al 1996).

The use of distant clusters is promising because it is a direct consequence of the detection of weak lensing signals, regardless of the accuracy of the mass reconstruction. The shape of the redshift distribution of the galaxies can be inferred if many clusters at different redshifts map the lensing signal. Up to now, the number of clusters is still low, but it will continuously increase during the coming years. However, it is worth noting that the derived shape of the redshift distribution also depends on the accuracy of the lens modeling, as well as on the dynamical evolution of clusters with look-back time. At high redshift it is possible that the lensing signal decreases rapidly, not only because of the absence of background sources, but also because clusters of galaxies are no longer dense and massive enough to produce gravitational distortion. It will be important to disentangle these two different processes.

The Distribution of Faint Galaxies From the Magnification Bias When the slope of the galaxy number count is lower than 0.3, a sharp decrease in the galaxy number density is expected close to the critical radius corresponding to the redshift of the background sources (see Equation 24). For a broad redshift distribution, the cumulative effect of each individual redshift results in a shallow depletion area which spreads over two limiting radii corresponding to the smallest and the largest critical lines of the populations dominating the redshift distribution. Therefore, the shape and the width of depletion curves reveal the redshift distribution of the background sources, and their analysis should provide valuable constraints on the distant galaxies. Similar to the lensing inversion, this is a statistical method that also needs a very good modeling of the lens; but in contrast to it, it does not need information on the shapes of arclets, so the "depletion-redshift" could be a more relevant approach for very faint objects.

This method was first used by Fort et al (1997) in the cluster Cl0024+1654 to study the faint distant galaxy population in the extreme magnitude ranges $B = 26.5$–28 and $I = 25$–26.5. The (unlensed) galaxy number counts were first calibrated using CFHT blank fields and checked from comparison with the HST-HDF counts. In this magnitude range, the slopes are close to 0.2, so these populations can produce a highly contrasted depletion area, so they are best suited for this project. In this cluster, the lower boundary of the depletion is sharp and the growth curve toward the upper radius extends up to 60 arcseconds from the cluster center, as expected if the high-redshift tail is a significant fraction of the lensed galaxies. Fort et al concluded that $60\% \pm 10\%$ of the B-selected galaxies are between $z = 0.9$ and $z = 1.1$ while most of the remaining $40\% \pm 10\%$ galaxies appear to be broadly distributed around a redshift of $z = 3$. The I selected population shows a similar bimodal distribution, but spreads up to a larger redshift range with about 20% above $z > 4$.

There is no spectroscopic confirmation yet that the double-shape redshift distribution predicted by Fort et al is real. Indeed, there are still uncertainties related to this method: in the particular case of Cl0024+1654, the redshift of the arc used to scale the mass was assumed to be close to 1. We know from recent Keck spectroscopic observation that this arc is at redshift 1.66 (Broadhurst et al 1999), so the innermost calibration of the sources has to be rescaled. The method is also sensitive to the lens modeling of the projected mass density. In the case of Cl0024+1654, it is rather well constrained from the subarcsecond ultra-deep images of Fort et al, and the predicted velocity dispersion is very close to the measured values from the galaxy radial velocities (Dressler & Gunn 1992).

This approach was recently generalized by Bézecourt et al (1998), in order to predict the number counts of arc(let)s with a magnification larger than a lower limit. The prediction first needs a model for galaxy evolution that reproduces some typical features of field galaxies, such as the observed galaxy counts and redshift distributions of spectroscopic surveys. The best final model can then be used to predict the number of arc(let)s brighter than a lower surface brightness limit and with magnification larger than a lower limit, for any lensing cluster whose mass distribution can be modeled properly. Bézecourt et al (1998, 1999) used this technique to build the best model capable of producing the number of arc(let)s observed in A370 and A2218. They also predicted a bimodal redshift distribution, but their expected number of giant arcs is overestimated by a factor of two. This inconsistency is still difficult to interpret. Indeed, the method should be handled carefully, because it both depends on the modeling of the lens and on the modeling of galaxy evolution. In particular, fitting of counts and redshift distributions of galaxies produces models that have degeneracies (Charlot 1999) that are potential limitations. Nevertheless, like the Fort et al (1997) method, the Bézecourt et al generalization is an interesting and original idea which can certainly be improved in the future using much better data. As compared with the lensing-inversion, it does not depend on the shapes of distant galaxies, and just needs very deep counts [the Bézecourt et al (1998, 1999) method does require shapes of lensed galaxies, but they only use reasonably magnified arc(let)s, so it is not a difficulty]. In the "depletion-redshift" technique this is a great advantage for the faintest (most distant?) objects, because, as the HDF images show, many of them have bright spots but do not show regular morphologies, so the lensing-inversion procedure could be inefficient for these galaxies. These very first attempts must be pursued on many lensing clusters in order to provide reliable results on the redshift distribution of the faintest galaxies.

The redshift distribution obtained by these various techniques is summarized in Figure 12. The distribution is broad and the comparison with Figure 9 of Fort & Mellier (1994) shows that the median redshift and the width of the distribution increases continuously. The median redshift distribution of giant arcs was close to 0.4 four years ago and has increased up to 0.7 but with a more pronounced high-redshift tail. A significant fraction of the new redshifts exceeds 1.5, with a visible trend toward very high redshifts ($z > 2.5$). The median redshift obtained from lensing inversions is close to 0.7, a good correlation with other methods. It

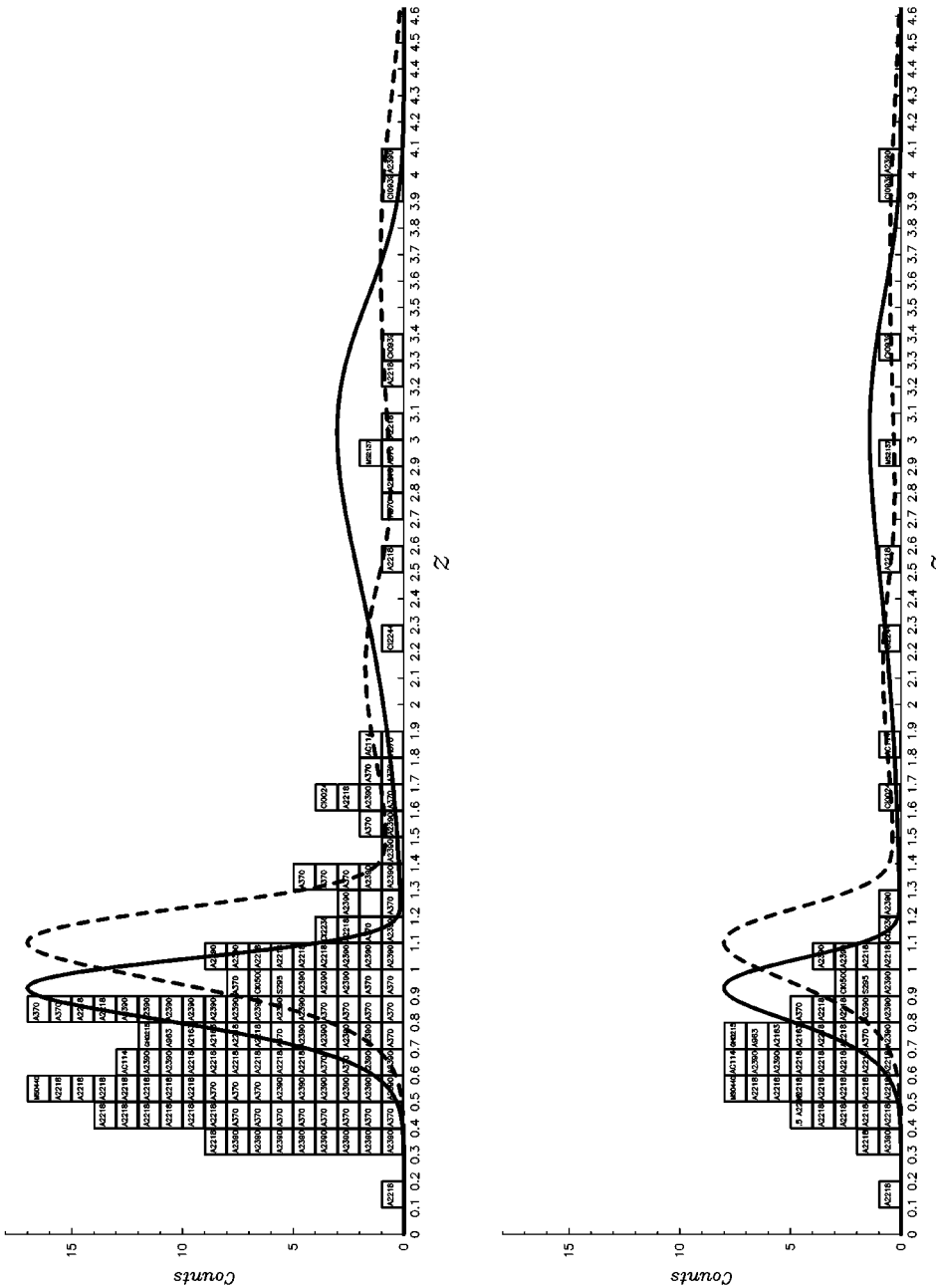
Counts
z
Counts
z

is surprising to see that the redshift distribution obtained by the depletion curves predict two peaks which seem to be visible in the redshift distribution of arc(let)s as well, both on the spectroscopic and lensing inversion samples. Owing to the somewhat different selection criteria used for these two samples, a resemblance was not really expected, and it may be an indication that selection biases in the spectroscopic sample of arc(let)s are not critical.

Because the observations of lensed galaxies simultaneously use magnification, color selection, shape selection (elongation) and relative position with respect to the cluster center (deviation angle), it is possible to jointly select drop-out galaxies with the radial-distance criterion of an elongated object in order to select extremely distant galaxies. Because this method seems to be efficient, it will certainly be applied to select samples of $z > 5$ galaxies. This will probably be a main goal for the future.

6.2 Spectral Content of Arc(let)s

The strong magnification of giant arcs also permits one to study the content and star formation rates of high-redshift galaxies. Preliminary studies started with Mellier et al (1991) and Smail et al (1993) who explored the spectral content of some arcs. These samples do not show spectacular starburst galaxies and seem to be compatible with a continuous star formation rate. The HST images confirm that many of these galaxies have bright spots with ongoing star formation. The star formation rates inferred from new optical spectra of arcs in A2390 (Bézecourt & Soucail 1996), in A2218 (Ebbels et al 1996), in Cl1358+6245 (Franx et al 1997) or in Cl0939 (Trager et al 1997) range from 5 to 20 $M_{\odot}$/yr and are consistent with other observations (Bechtold et al 1998), but none of the rates computed for arclets are corrected from dust extinction.

It is only very recently that the material of magnified arcs has been studied in detail. Trager et al (1997) made the first attempt to estimate the metallicity of the arclets at $z > 3$ detected in Cl0939 with the Keck telescope, and found that they are metal-poor systems, having $Z < 0.1\ Z_{\odot}$. The very first CO observations at IRAM of the giant arc in A370 [Casoli et al 1996: CO(J=2-1) detected] and at Nobeyama Observatory in MS1512-cB58 [Nakanishi et al 1997: CO(J=3-2) undetected] have demonstrated that (sub)millimeter observations are feasible thanks to the magnification and can provide useful diagnoses on the molecular and gas content of galaxies at high redshifts. If, as suggested by the cosmic infrared background (Puget et al 1996; see also Guiderdoni 1998 and references therein), a significant fraction of the UV emission of distant galaxies is released in the

Figure 12 Redshift distribution inferred from lensing techniques. The bottom panel is the spectroscopic sample of arc(let)s compiled from the literature. The top panel includes the spectroscopic sample and the redshift predictions of arclets from lensing inversion. On both histograms, the plots of the redshift distributions from the depletion curves in B (*solid line*) and I (*dashed line*) prediction by Fort et al (1997) are shown.

submillimeter range, the observations of lensed galaxies in the submillimeter and millimeter bands could be a major step in our understanding of the history of star formation in galaxies. Blain (1997) emphasized that the joint submillimeter flux-density/redshift relation and the steep slope counts make the observations of lensed distant galaxies in this waveband an optimum strategy, so a large number of bright (magnified) sources are expected. Both SCUBA (at 450 μm and 850 μm) and IRAM (at 1.3 mm) can therefore benefit from magnification of distant lensed galaxies. The large field of view and the wavelength range of SCUBA at JCMT seem perfectly suited for this program. Smail et al (1997b) are carrying out a long-term program of observations of lensing clusters with this instrument. They detected sources in A370 and Cl2244-02 with a success rate which implies that the number density of these galaxies is about 3 times higher than expected from the 60 μm IRAS count. Their observations of a new sample of 7 lensing clusters (Smail et al 1999) show that the energy emitted by these galaxies is much higher than the expectations from nearby galaxies. Most of these galaxies are at redshift larger than 1, and probably less than 5.5. The star formation activity of high-redshift galaxies is therefore important, and for those which have an optical counterpart, their morphology reveals signs of merging processes. Therefore, the star formation activity seems frequently triggered by interactions (Smail et al 1999), which corroborates the recent ISOCAM observations in some giant arcs, as in A2390 (Lémonon et al 1998). The star formation rates measured from the various fluxes have a very broad range, between 50 to 1000 $M_{\odot}$/yr, but they are difficult to estimate accurately, in particular for the hyperluminous system in A370 (Ivison et al 1998) because AGNs could contribute significantly to the flux.

The submillimeter observation is certainly one of the most promising tools for the future. The magnification and the shape of the continuum produced by dust make the "submillimeter gravitational telescope" perfect for studying the high-redshift Universe and the star formation history of galaxies.

6.3 Morphology of Highly Magnified Galaxies

Although the coupling of gravitational telescopes with the high resolution images from HST is superb for probing the intrinsic morphology of arc(let)s, no significant results have been raised from recent studies. Many HST images of arcs are made of two parallel elongated arcs, as in A2390 (Kneib et al, in preparation) or in MS2137-23 (Hammer et al 1997; see arcs A and C in MS2137-23 in Figure 3), which supports the idea that these distant galaxies are interacting systems, as it was reported in the previous section. Other images show bright spots which are interpreted as star forming regions, like Cl2244-02 (Hammer & Rigaud 1989), A2390 (Pelló et al, in preparation) or Cl0024+1654 (Colley et al 1996). In the case of the giant arc in Cl1358+62 at $z = 4.92$, the comparion of the visible and the near-infrared observations obtained with the HST and the Keck telescopes (Soifer et al 1998) reveals that one of its bright spots already contains half the stellar mass of the galaxy. It shows that at this redshift, galaxies may already have dense cores.

Furthermore, the visible and near infrared imaging and spectrospic data show also that reddening produced by dust is important, even at that redshift.

The detailed description of a $z \approx 5$-galaxy given by Soifer et al strengthens the usefulness of image reconstruction techniques of high-redshift lensed galaxies, as the one initially proposed by Kochanek et al (1989). Some attempts have already been made in Cl0024+1654 (Wallington et al 1995, Colley et al 1996) or in MS2137-23 (Hammer et al 1997). They succeed in reproducing a single image in the source plane, but the details of the morphology are still uncertain and do not yet provide valuable information on distant galaxies. Therefore, it is still premature to present quantitative results on the distant galaxies, first because this sample is poor and incomplete, and second because there are too many uncertainties in the source reconstruction.

7. COSMOLOGICAL PARAMETERS

The potential of gravitational lensing for cosmography, already discussed by Blandford & Narayan (1992) and Fort & Mellier (1994) for the particular cases of arc(let)s, is clear but also challenging. The increasing evidence that the whole set of observations are compatible with a non-zero cosmological constant, for instance, motivated many new studies devoted to the constraints on λ, following the early suggestions by Paczynski & Gorski (1981). One of the most promising and reliable approaches explored by recent theoretical studies has been raised by Bernardeau et al (1997) and Van Waerbeke et al (1999). These works clearly demonstrate that the determination of the cosmological parameters (Ω_0, λ) using future surveys of weak lensing induced by large-scale structures should provide Ω with a high accuracy (see Figure 7 and Figure 13). Since this was already pointed out in Section 4.1, I do not discuss it in more detail here. In the following sections, I focus on new and more speculative investigations, which are still difficult to implement but seem promising in the future.

7.1 Constraints from Cluster Reconstruction

Following the early suggestion by Paczynski & Gorski (1981) for multiply imaged quasars, Breimer & Sanders (1992) (see also Fort & Mellier 1994, Link & Pierce 1998) emphasized that the ratio of angular diameter distances of arc(let)s having different redshifts does not depend on the Hubble constant and therefore can constrain (Ω, λ). This ratio still depends on the mass distribution within the two critical lines corresponding to redshifts z_1 and z_2, so it is worth noting that it is sensitive to the modeling of the lens. It is only in the case of an isothermal sphere model that the radial positions of the critical lines θ, where arcs at a given redshift are formed, only depend on the angular distances $D(z_s, \Omega_0, \lambda)$:

$$\left(\frac{\theta_1}{\theta_2}\right) = \left(\frac{D_{LS}(z_1, \Omega_0, \lambda)}{D_{OS}(z_1, \Omega_0, \lambda)}\right)\left(\frac{D_{OS}(z_2, \Omega_0, \lambda)}{D_{LS}(z_2, \Omega_0, \lambda)}\right). \tag{40}$$

Because cluster potentials are by far more complex than isothermal spheres, in practice the method works only for very specific cases, such as clusters with regular morphology, and if auxiliary independent data, such as high-quality X-ray images or additional multiple images, help to constrain the lens model. So far, no case has been found where the modeling of two (or more) arc systems at very different redshifts is sufficiently reliable. However, the joint HST images and spectroscopic redshifts obtained with new giant telescopes should provide such perfect configurations in the near future. A1689 or MS0440 seem like good examples of such candidates because both show many arc(let)s and have a regular shape.

A similar approach has been proposed by Hamana et al (1997), using the arc cB58 observed in the lensing cluster MS1512.4+3647. Assuming that the dark matter distribution is sufficiently constrained by the ROSAT and ASCA data, the magnification and number of multiple images of cB58 only depend on the cosmology. One should therefore use the detection of counter-image to cB58 to constrain the domain (Ω_0, λ) which cannot produce a counter-arc. This point was discussed by Seitz et al (1997) who argue that in practice it cannot work because it depends too much on the modeling of the lensing cluster. The variation of the lensing strength as a function of cosmology is small, lower than 0.5% between an EdS universe and an $\Omega = 0.3,\ \lambda = 0$ universe. Furthermore, the use of independent X-ray data to model the dark matter demands a very good understanding of the physics of the hot gas for each individual cluster considered.

More recently, Lombardi & Bertin (1999) have proposed the use of weak lensing inversion to recover simultaneously the cluster mass distribution and the geometry of the universe. The method assumes that the redshifts of the lensed galaxies are known. In that case, for a given cosmology, it is possible to compute the shear at a given angular position which is produced on a lensed galaxy located in a narrow redshift range, from the observed ellipticities of the galaxies at that angular position. Conversely, if the shear is known, then it is possible to infer the best set of cosmological parameters which reproduce the observed ellipticities of the galaxies. Therefore, it is possible to iterate a procedure, starting from an arbitrary guess for the set (Ω, λ), which at the final step will simultaneously procure the best mass inversion with the most probable (Ω, λ). The key point is the assumption that the redshift of each individual source is known. The method should provide significant results if at least a dozen of clusters with different redshift are reconstructed using this iterative procedure (Lombardi & Bertin 1999). Indeed, this inversion is demanding in telescope time since a very good knowledge of the redshifts of many lensed sources is necessary; but otherwise the method seems promising.

7.2 Statistics of Arc(let)s

Up to now, several tens of multiply imaged distant galaxies have already been detected in clusters of galaxies, and this number will probably increase by a large factor within the next few years. Since the fraction of rich clusters (and

therefore lensing-clusters) strongly depends on the cosmological scenario, we expect the number of arc(let)s to depend on cosmological parameters (Wilson et al 1996b).

It is well known that present-day statistical studies of clusters of galaxies are limited by the few samples of cluster catalogs with well understood selection function. Wu & Mao (1996) analyzed the statistics of arcs in the EMSS cluster sample (Gioia et al 1990) and show that the fraction is twice the one expected for an EdS Universe, but compatible with a flat $\lambda = 0.7$ model (see also Cooray 1999). Unfortunately, the geometry of the mass distribution and the substructures present in the lensing cluster increase the shear contribution to the magnification and change dramatically the expected number of arcs (Bartelmann et al 1995, Bartelmann 1995b, Hattori et al 1997, Bartelmann et al 1998). The importance of accurate simulations of clusters is clearly obvious from the recent studies. Bartelmann et al (1998) find a totally opposite result to that of Wu & Mao, and conclude that an open model ($\Omega = 0.3$ and $\lambda = 0$) is preferred to any flat models to reproduce the number of arcs observed. The other models, including the $\lambda = 0.7$ model, fail by about of factor of ten. This is a clear demonstration that the use of statistics of arc(let)s to constrain the cosmological scenario is very sensitive to the assumptions. The constraint on λ from the fraction of arc(let)s is therefore rather weak and hopeless for the moment.

7.3 Magnification Bias

The depletion of the galaxy number density as a function of radial distance from the cluster center can potentially provide information on the cosmological constant. The reason for this is ultimately the same as for giant arcs—namely, the ratios of angular distances which strongly depend on the cosmological constant. Therefore, if the redshift distribution of the sources and the mass distribution of the lensing cluster are known, the shape of the depletion curve—in particular, its extension at a large radius—is constrained by λ.

Fort et al (1997) have used this property in order to constrain the cosmological constant. They used ultra-deep images of the lensing clusters Cl0024+1654 and A370 which permit a good signal to noise ratio of the depletion curves. These clusters have giant arcs with known redshift so the mass at a given critical line can be scaled. The method provides jointly the redshift of the sources and the cosmological parameters. Fort et al (1997) found that the location of this high redshift critical line rather favors a flat cosmology with λ greater than 0.6.

It is remarkable that from these two clusters only the method predicts a value of λ compatible with other independent approaches (see White 1998 and references therein). Since it needs a good model for the lens, this method has still many uncertainties and can be significantly improved with a large sample of arc clusters, in particular by using a maximum likelihood analysis applied to the probabilities of reproducing their observed local shears and convergences. A strong improvement can come from the new possibility of using the redshift distribution

found independently. This should be possible using photometric redshifts. Even more promising, Gautret et al (1998) proposed to use triplets of neighbouring arclets at a different redshift. Because they are close together, the positions of these arclets are independent of the mass profile but only depend on λ. This in principle breaks the degeneracy and solves this problem.

All the methods described above do not yet provide convincing results on λ mainly because they use simultaneously different quantities which are degenerate without external information: mass distribution of the lensing-cluster, redshift distribution of the sources, cosmological parameters, and evolution scenarios of clusters and of sources. The approach using statistics of arc(let)s looks promising but demands very good simulations and a good understanding of selection functions of cluster samples which are used for comparison with observations. The method using lens modeling requires very good lens models and information on the redshift distribution of galaxies, in particular for the most distant ones, since they contain the population which depends the most on λ. This approach can use the redshift distribution obtained from photometric redshifts, and should focus on regular lensing clusters containing giant arcs with known redshift. As emphasized by Fort et al (1997), Lombardi & Bertin (1999) and Gautret et al (1998), significant results cannot be expected until many clusters have been investigated. This should be done within the next few years, in particular using 10-meter class telescopes. However, it is remarkable that the Fort et al limit corresponds to the value given by Im et al (1997) from the measurement of strong lensing produced by elliptical galaxies, and to the upper limit given by Kochanek (1996) from the statistics of lensed quasars.

8. LENSING THE CMB

The measurement of CMB fluctuations is a major goal for cosmology in the next decade (see White et al 1994, and references therein). The shape of the power spectrum over the whole spectral range contains a huge amount of information which permits one to constrain the cosmological scenario with an incredibly high accuracy. However, the reliability of the interpretation of the features visible on the spectrum requires a complete and detailed understanding of all the physical mechanisms responsible for its final shape. Gravitational lensing induced by foreground systems along the line of sight may play a role, so it is important to predict in advance whether it can modify the signal from the CMB and, if so, what the expected amplitudes of the effects are.

Because surface brightness is conserved by the gravitational lensing effect (Etherington 1933), only fluctuations of the CMB temperature maps can be affected by lensing. However, even for strong lenses, no significant modification of the power spectrum is expected on large scales (Blanchard & Schneider 1987) and therefore there is no hope of detecting positive signals of the coupling between CMB and gravitational lensing in the Cosmological Background Explorer (COBE)

maps. Nevertheless, since the COBE-Differential Microvawe Radiometer (DMR) experiment has demonstrated that fluctuations exist (Smooth et al 1992), the study of the lensing effect on smaller scales than COBE resolution is potentially interesting and has some advantages with respect to weak lensing on distant galaxies. First, contrary to lensed galaxies, the redshift of the source, namely the last scattering surface, is well known and spreads over a very small redshift range. Second, with the on-going and the coming of high-resolution ground-based and balloon observations as well as the two survey satellites MAP and Planck-Surveyor, observation of low-amplitude temperature distortions on small scales will become possible and will permit investigation of possible lensing effects.

Early theoretical expectations from Blanchard & Schneider (1987) or Cole & Efstathiou (1989) show that the *shape* of the small-scale temperature fluctuations can be modified by lensing effects; in particular they can redistribute the power in the power spectrum. In contrast, the *amplitude* of the temperature anisotropy on medium and small scales has been a matter of debates during the last decade (see the review by Blandford & Narayan 1992, and more recently Fukushige & Makino 1994; Fukushige et al 1994; Cayón et al 1993a,b, 1994). The conclusions of these works showed strong discrepancies, depending on the assumptions used to explore the deflection of photons and to model inhomogenous universes. Furthermore, the expectation values also depend on the cosmological models. Indeed, the most recent critical studies show that the effect of lensing on large scales is negligible (Seljak 1996, Martínez-González et al 1997). In particular, the non-linear evolution of the power spectrum does not significantly increase the amplitude on these scales. On the other hand, the gravitational lensing effect reduces the power spectrum on small scales, and eventually can smooth out acoustic peaks on scales below $l \approx 2000$ (Seljak 1996). Martínez-González et al (1997) obtained conclusions similar to those of Seljak—that is, the contribution of lensing is small but not negligible and should be taken into account in the detailed analysis of future CMB maps. Furthermore, the transfer of power from large to small scales induces an important increase of power in the damping tail, which results in a decrease of very small scale amplitudes at a smaller rate than expected without lensing (Metcalf & Silk 1997, 1998). According to Metcalf & Silk (1997), 30% of the additional power at $l = 3000$ comes from $l < 1000$ scales, and 8% from $l < 500$ in the case of a $\sigma_8 = 0.6$, $h = 0.6$ model.

Zaldarriaga & Seljak (1998) pointed out that gravitational lensing not only smoothes the temperature anisotropy, but can also change the polarization. The polarization spectra are more sensitive to gravitational lensing effects than the power spectrum of the temperature because the acoustic oscillations of polarization spectra have sharper oscillations and can be smoothed out more efficiently by lensing than temperature fluctuations. The effect is small but can reach amplitudes of approximately 10% for $l < 1000$ scales. More remarkably, because of the coupling between E-type and B-type polarizations (Seljak 1997b), gravitational lensing can generate low amplitude B-type polarization, even if none is predicted from primary fluctuations (for instance, for scalar perturbations).

Because the signal is weak and only concerns the small scales, temperature and polarization fluctuations induced by gravitational lensing will be difficult to measure with high accuracy and seems a hopeless task before the Planck-Surveyor mission. It is therefore valuable to explore alternatives which could provide better or complementary information which couples lensing and CMB. An interesting idea is to analyze the non-Gaussian features induced by the displacement fields generated by gravitational lensing on the CMB maps (Bernardeau 1997, 1998b). As for weak lensing on distant galaxies, the CMB temperature map can be sheared and magnified. The resulting distortion patterns are direct signatures of the coupling between the CMB and the foreground lenses. Bernardeau (1998b) argued that the distortion map produced by lensing can be decoupled from other fluctuation patterns because it generates similar magnification and deformation on close temperature patches, which therefore can be correlated. He also explored the consequences of the non-Gaussian signal on the four-point correlation function. Unfortunately, the signal is very small, and it is even not clear on which scale the signal is highest, in particular because the non-linear evolution of the power spectrum was not considered by Bernardeau. The weakness of the signal and the fact that the four-point correlation function could be contaminated by other non-Gaussian features are strong limitations of Bernardeau's suggestion. Therefore, Bernardeau (1998b) preferred to focus on the modification of the ellipticity distribution function of the temperature patches induced by lensing. From his simulated lensed maps, a clear change of the topology of the temperature maps is visible: the shapes of the structures are modified and their contours look sharper than for the unlensed maps. However, the signal is still marginally detectable on a $10^\circ \times 10^\circ$ map, even with Planck-Surveyor.

From these investigations it is clear that weak lensing on the CMB has small effects on the spectrum of the temperature and polarization power spectra and on the non-Gaussianity of the CMB temperature maps. However, with typical amplitude of 1% to 10% percent they can be detected with future missions, so they must be taken into account for detailed investigations of the CMB anisotropy on small scales. This is an important prediction since the detection of gravitational lensing perturbations of the CMB will be possible with Planck-Surveyor. Its high sensitivity and spatial resolution are sufficient to permit one to break the geometrical degeneracy expected from linear theory, and to disentangle different (Ω, λ) common models (Metcalf & Silk 1998; Stompor & Efstathiou 1999). It is worth noting that these analyses can be used jointly with the weak lensing maps of large-scale structures on background galaxies which will also provide (Ω, λ) with a very good accuracy.

9. FUTURE PROSPECTS

Although the use of weak lensing analysis and its applications in cosmology made spectacular progress during the last five years, most of the astrophysical questions addressed by Fort & Mellier (1994) in their conclusions are still pending.

However, it seems that we are progressing quickly in the right direction, even if some of these problems are complex and should be envisioned in a long-term perspective.

The HST images have dominated most of the results, in particular in the modeling of clusters of galaxies. Thanks to the formidable work devoted to mass reconstruction, the projected mass density of clusters of galaxies are now robust and reliable. It is now important to couple strong and weak lensing features (Seitz et al 1998, AbdelSalam et al 1998b, Dye & Taylor 1998, Van Kampen 1998) in order to build consistent models for clusters. It is worth noting that for many of the issues discussed in this review, it was emphasized that precise and reliable mass reconstructions of clusters of galaxies are crucial and determine the reliability of many scientific outcomes. In this respect, it is important to keep in mind that the redshift distribution of the sources is indispensable and that the new giant telescopes will be the best tools for this purpose.

From the sample of clusters already analyzed, there are converging results that $\Omega < 0.3$ with a high confidence level. However, complete cluster samples are necessary for deeper investigations of cluster properties. They should come out rapidly from weak lensing studies of ROSAT samples (Rosati 1999). Indeed, we now have a very good understanding of the mass distribution of each component (dark matter, hot gas, galaxies) in clusters of galaxies and we are close to understanding the discrepancy between the lensing mass and the X-ray mass of clusters. During the next five years, one can reasonably expect significant improvements in our knowledge of the dynamics of clusters of galaxies by jointly using weak lensing reconstruction, from HST and giant telescopes images, and a full description of the hot gas, from AXAF and XMM observations.

In contrast, the investigation of galaxy halos from galaxy-galaxy lensing is still in its infancy and the preliminary results presented in this review must be confirmed. A new generation of instruments will contribute to the development of this hot topic. Below 10 arcseconds down to 2 arcseconds, "wide field" HST observations with the new Advanced Camera devoted to deep galaxy-galaxy lensing studies appear to be a promising approach. Beyond this scale, the high image quality of telescopes like Keck, GEMINI, Subaru, Magellan, the VLT or CFHT will be decisive in obtaining valuable constraints from galaxy-galaxy lensing analysis between 10 and 60 arcseconds.

Parallel to these studies, we can now envision fully exploiting some of the most valuable information that gravitational lensing can provide, namely the relation(s) between light and mass distributions in the universe. Theoretical studies have demonstrated that in the near future the weak lensing analysis coupled with the study of the galaxy distribution will allow us to understand the evolution of the biasing factor with scale and redshift. However, it is important to explore the case of non-linear and stochastic biasing in order to understand which parameters can be reasonably constrained. The possible existence of large dark halos around galaxies or in clusters of galaxies is also an unknown but fascinating topic. In this respect, the dark cluster candidates discussed by Hattori et al (1997) and Erben et al (1999), or the remarkable distortion field detected by Bonnet et al (1994) in

the periphery of Cl0024+1654, which does not seem to be correlated to luminous matter, deserves more careful investigation.

The study of the contents and the past history of galaxies made formidable progress as well. It is clear that jointly using the magnification of cluster-lenses with the unprecedented image quality of HST, or with the wide field and high sensitivity of SCUBA, results in highly competitive tools. In the future, continuous developments are expected, but the observation of extremely high redshift galaxies which could not be observed without magnification is certainly a major goal, in particular in the submillimeter wavebands. As demonstrated by the recent study of Soifer et al (1998), the coming of optical and near-infrared spectroscopic capabilities on the giant telescopes will permit one to study in detail their spectral energy distribution and the kinematics of their stellar and gas components. The magnification permits the viewing of a huge amount of detail on the images of these galaxies, and we can envision probing small details of these galaxies from image reconstruction "à la Kochanek" (Kochanek et al 1989). Unfortunately, though theoretical tools have been developed in order to recover the morphology of these lensed galaxies, the quality of optical and submillimeter data are not good enough to produce reliable details of the sources from inversion. This is probably a goal for the Large Southern Array (LSA) which will have much better sensitivity and resolution.

With new instruments, such as Megacam at CFHT (Boulade et al 1998) or the VST at the European Southern Observatory (Arnaboldi et al 1999) in Paranal, we are now entering the era of wide field subarcsecond imaging surveys which will produce the first shear-limited samples or, similarly, the first mass selected catalogues of gravitational condensations (Reblinsky & Bartelmann 1999). Their designs are optimized to investigate weak lensing induced by large-scale structures in order to produce the first mass maps of the universe. They will permit recovering of the detailed spectrum of the projected power spectrum of mass density fluctuations as well as measuring (Ω, λ) with an accuracy greater than 10% (see Figure 13, color). There are still some theoretical issues (see Sections 3.3 and 4.4) that must be addressed in detail from both the theoretical and simulation points of view. For most of them, there are no crucial conceptual difficulties, so they should be fixed rapidly. On the other hand, the control of systematics which can affect weak lensing measurement, as well as the correction for an anisotropic PSF, could be critical and should be considered seriously in the future for very low shear amplitudes ($<1\%$). Nevertheless, these cameras, as well as the very wide field surveys of the VLA-FIRST and the SDSS, should provide a major breakthrough in weak lensing applications for cosmology.

In the longer term, after the crucial results expected for mass maps with wide-field CCD cameras, the New Generation Space Telescope (NGST) and Planck Surveyor could be ultimate steps in this area. The potential interest of NGST for weak lensing has been summarized by Schneider & Kneib (1998), who argued that low-mass clusters and groups of galaxies as well as very distant clusters should be detectable with this telescope. In parallel, as reported by Stompor & Efstathiou (1998) and Metcalf & Silk (1998), weak lensing on the CMB should

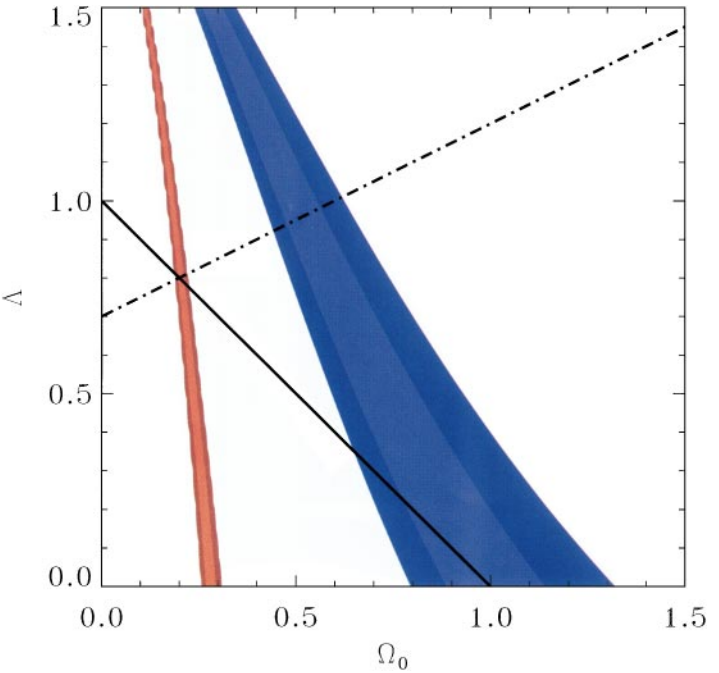

Figure 13 Constraints on (Ω, λ) from a weak lensing survey covering 10×10 square-degrees. The bright and dark regions refer to 1σ and 2σ level. The left strip is for an $\Omega = 0.3$ universe, and the right band for an $\Omega = 1$ universe. The solid and dot-dashed lines correspond to a zero-curvature universe and to a fixed deceleration parameter, respectively (from Van Waerbeke et al 1999).

be able to break the geometrical degeneracy and ultimately provide the (Ω, λ) parameters. This coupling between observations of CMB fluctuations and weak lensing analyses emerges as a consecration illustrating the major roles played by these two complementary approaches to present-day cosmology.

ACKNOWLEDGMENTS

I am particularly grateful to B. Fort for his advices, and his friendly and continuous encouragements during the long period of preparation of the review. I would like to thank first F Bernardeau, F Casoli, S Charlot, R Ellis, P Schneider and L Van Waerbeke for their careful reading and useful comments of the manuscript as well as for their strong support during its writing. I thank all the other close collaborators who participate to our gravitational lensing projects, and the colleagues with whom we had many fruitful discussions, namely M Bartelmann, H Bonnet, T Broadhurst, J-C Cuillandre, T Erben, H Hoekstra, B Jain, N Kaiser, J-P Kneib, C Kochanek, J-F Le Borgne, P-Y Longaretti, G Luppino, D Narasimha, R Pelló, M Pierre, C Seitz, S Seitz, U Seljak, I Smail, G Soucail and G Squires. I thank I Gioia for providing me data prior to publication, and T Brainerd, B Jain, P Schneider and G Squires, for giving me their authorization to publish figures of their papers in this review. I thank especially M Dantel-Fort for her assistance and also for the crucial work she does in order to have all these data set ready for our scientific objectives. Part of this work was supported by the Programme National de Cosmologie which is funded by the Centre National de la Recherche Scientifique, the Commissariat à l'Énergie Atomique and the Centre National d'Études Spatiales, under the responsibility of the Institut National des Sciences de l'Univers and the Indo-French Centre for the Promotion of Advanced Research IFCPAR grant 1410-2.

LITERATURE CITED

AbdelSalam HM, Saha P, Williams LLR. 1998a. *MNRAS* 294:734–46

AbdelSalam HM, Saha P, Williams LLR. 1998b. *Astron. J.* 116:1541–52

Allen SW. 1998. *MNRAS* 296:392–406

Amram P, Sullivan WT, Balkowski C, Marcelin M, Cayatte V. 1993. *Ap. J. Lett.* 403:L59–62

Arnaboldi M, Capaccioli M, Mancini D, Rafanelli P, Sedmak G, Scaramella R, Vettolani GP. 1999. In *Wide Field Surveys in Cosmology*, ed. S Colombi, Y Mellier, B Raban. Paris: Frontières

Babul A, Lee MH. 1991. *MNRAS* 250:407–13

Bar-Kana R. 1996. *Ap. J.* 486:17–27

Bartelmann M. 1995a. *Astron. Astrophys.* 298:661–71

Bartelmann M. 1995b. *Astron. Astrophys.* 299: 11–16

Bartelmann M. 1995c. *Astron. Astrophys.* 303: 643–55

Bartelmann M. 1996. *Astron. Astrophys.* 313: 697–702

Bartelmann M, Narayan R. 1995. *Ap. J.* 451:60–75

Bartelmann M, Narayan R, Seitz S, Schneider P. 1996. *Ap. J. Lett.* 464:L115–18

Bartelmann M, Schneider P. 1993a. *Astron. Astrophys.* 268:1–13
Bartelmann M, Schneider P. 1993b. *Astron. Astrophys.* 271:421–24
Bartelmann M, Schneider P. 1994. *Astron. Astrophys.* 284:1–11
Bartelmann M, Schneider P, Hasinger G. 1994. *Astron. Astrophys.* 290:399–411
Bartelmann M, Steinmetz M, Weiss J. 1995. *Astron. Astrophys.* 297:1–12
Bartelmann M, Huss A, Colberg JM, Jenkins A, Pearce FR. 1998. *Astron. Astrophys.* 330:1–9
Bechtold J, Elston R, Yee HKC, Ellingson E, Cutri RM. 1998. In *The Young Universe*, ed. S D'Odorico, A Fontana, E Giallongo, pp. 241–48. PASP Conf. Series. Vol. 146
Benítez N, Martínez-González E. 1997. *Ap. J.* 477:27–35
Bernardeau F. 1997. *Astron. Astrophys.* 324:15–26
Bernardeau F. 1998a. *Astron. Astrophys.* 338: 375–82
Bernardeau F. 1998b. *Astron Astrophys.* 338: 767–76
Bernardeau F, Van Waerbeke L, Mellier Y. 1997. *Astron. Astrophys.* 322:1–18
Bézecourt J, Soucail G. 1997. *Astron. Astrophys.* 317:661–69
Bézecourt J, Pellé R, Soucail G. 1998. *Astron. Astrophys.* 330:399–411
Bezecourt J, Kneib J-P, Soucail G, Ebbels TMD. 1999. *Astron. Astrophys.* 347:21–29
Bingelli B. 1992. *Astron. Astrophys.* 107:338–49
Blain A. 1997. *MNRAS* 290:553–65
Blanchard A, Schneider J. 1987. *Astron. Astrophys.* 184:1–6
Blandford RD. 1990. *Q. Jl. R. Astron. Soc.* 31:305–31
Blandford RD, Jaroszyński M. 1981. *Ap. J.* 246:1–12
Blandford RD, Saust AB, Brainerd TG, Villumsen JV. 1991. *MNRAS* 251:600–27
Blandford RD, Narayan R. 1992. *Annu. Rev. Astron. Astrophys.* 30:311–58
Bonnet H, Fort B, Kneib J-P, Mellier Y, Soucail G. 1993. *Astron. Astrophys. Lett.* 280:L7–10
Bonnet H, Mellier Y, Fort B. 1994. *Ap. J. Lett.* 427:L83–86
Bonnet H, Mellier Y. 1995. *Astron. Astrophys.* 303:331–44
Böhringer H, Tanaka Y, Mushotzky RF, Ikebe Y, Hattori M. 1998. *Astron. Astrophys.* 334:789–98
Boulade O, Vigroux L, Charlot X, de Kat J, Borgeaud P, Roussé JY, Mellier Y, Gigan P, Crampton D. 1998. *Astronomical Telescopes and Instrumentation.* SPIE Vol. 3355
Bouchet F. 1996. Preprint astro-ph/9603013
Bower RG, Smail I. 1997. *MNRAS* 290:292–302
Brainerd TG, Blandford RD, Smail I. 1996. *Ap. J.* 466:623–37
Breimer TG, Sanders RH. 1992. *MNRAS* 257:97–104
Bridle SL, Hobson MP, Lasenby AN, Saunders R. 1998. *MNRAS* 299:895–903
Broadhurst T. 1995. Preprint astro-ph/9511150
Broadhurst T, Taylor AN, Peacock J. 1995. *Ap. J.* 438:49–61
Canizares CR, 1981. *Nature* 291:620–24
Casoli F, Encrenaz P, Fort B, Boissé P, Mellier Y. 1996. *Astron. Astrophys. Lett.* 306:L41–44
Cayón L, Martínez-González E, Sanz JL. 1993a. *Ap. J.* 403:471–75
Cayón L, Martínez-González E, Sanz JL. 1993b. *Ap. J.* 413:10–13
Cayón L, Martínez-González E, Sanz JL. 1994. *Astron. Astrophys.* 284:719–23
Charlot S. 1999. In *The Next Generation Space Telescope: Science Drivers and Technological Challenges*, ed. P Benvenuti et al. ESA SP-429
Clowe D, Luppino GA, Kaiser N, Henry JP, Gioia IM. 1998. *Ap. J. Lett.* 497:L61–64
Cole S, Efstathiou G. 1989. *MNRAS* 239:195–200
Colombi S, Szapudi I, Szalay A. 1998. *MNRAS* 296:253–74
Colley WN, Tyson JA, Turner E. 1996. *Ap. J. Lett.* 461:L81–86
Connolly AJ, Csabai I, Szalay A, Koo DC, Kron RG, Munn JA. 1995. *Astron. J.* 110:2655–64

Cooray AR. 1999. *Astron. Astrophys.* 341:653–61
Coutts A. 1996. *MNRAS* 278:87–94
Cuillandre J-C, Mellier Y, Dupin J-P, Tilloles P, Murowinski R, Crampton D, Woof R, Luppino GA. 1996. *Pub. Astron. Soc. Japan* 108:1120–28
Dekel A, Lahav O. 1998. Preprint astro-ph/9806193
Dell'Antonio IP, Tyson JA. 1996. *Ap. J. Lett.* 473:L17–20
Deltorn J-M, Le Fèvre O, Crampton D, Dickinson M. 1997. *Ap. J. Lett.* 483:L21–24
Dolag K, Bartelmann M. 1997. *MNRAS* 291:446–54
Donahue M, Voit M, Gioia IM, Hughes J, Stocke J. 1998. *Ap. J.* 502:550–57
Dressler A, Gunn JE. 1992. *Ap. J. Supp.* 78:1–60
Dressler A, Oemler A, Sparks WB, Lucas RA. 1994. *Ap. J. Lett.* 435:L23–26
Dye S, Taylor A. 1998. *MNRAS* 300:L23–28
Ebbels T, Le Borgne J-F, Pelló R, Ellis RS, Kneib J-P, Smail I, Sanahuja B. 1996. *MNRAS* 281:75–81
Ebbels T, Le Borgne J-F, Pelló R, Ellis RS, Kneib J-P, Smail I, Sanahuja B. 1998. *MNRAS* 295:75–91
Ellis RS. 1997. *Annu. Rev. Astron. Astrophys.* 35:389–444
Erben T, Van Waerbeke L, Mellier Y, Schneider P, Cuillandre J-C, Castander F, Dantel-Fort M. 1999. Preprint astro-ph/9907134
Etherington IMM. 1933. *Phil. Mag.* 15:761–75
Evans NW, Wilkinson MI. 1998. *MNRAS* 296:800–12
Fahlman G, Kaiser N, Squires G, Woods D. 1994. *Ap. J.* 437:56–62
Fischer P, Tyson JA. 1997. *Astron. J.* 114:14–24
Fischer P, Tyson JA, Bernstein GM, Guhathakurta P. 1994. *Ap. J. Lett.* 431:L71–74
Fischer P, Bernstein G, Rhee G, Tyson JA. 1997. *Astron. J.* 113:521–30
Fort B, Prieur J-L, Mathez G, Mellier Y, Soucail G. 1988. *Astron. Astrophys. Lett.* 200:L17–20
Fort B, Le Fèvre O, Hammer F, Cailloux M. 1992. *Ap. J. Lett.* 399:L125–29
Fort B, Mellier Y. 1994. *Astron. Astrophys. Rev.* 5:239–92
Fort B, Mellier Y, Dantel-Fort M, Bonnet H, Kneib J-P. 1996. *Astron. Astrophys.* 310:705–14
Fort B, Mellier Y, Dantel-Fort M. 1997. *Astron. Astrophys.* 321:353–62
Franx M, Illingworth GD, Kelson DD, Van Dokkum PG, Tran K-V. 1997. *Ap. J. Lett.* 486:L75–78
Frye BL, Broadhurst TJ. 1998. *Ap. J. Lett.* 499:L115–18
Frye BL, Broadhurst TJ, Spinrad H, Bunker A. 1998. In *The Young Universe*, ed. S D'Odorico, A Fontana, E Giallongo, pp. 182–85. PASP Conf. Series. Vol. 146
Fugmann W. 1990. *Astron. Astrophys.* 240:11–21
Fukushige T, Makino J. 1994. *Ap. J. Lett.* 436:L111–14
Fukushige T, Makino J, Ebisuzaki T. 1994. *Ap. J. Lett.* 436:L107–10
Garrido JL, Battaner E, Sánchez-Saavedra ML, Florido E. 1993. *Astron. Astrophys.* 271:84–88
Gautret L, Fort B, Mellier Y. 1998. Preprint astro-ph/9812388
Geiger B, Schneider P. 1998. *MNRAS* 295:497–510
Geiger B, Schneider P. 1999. *MNRAS* 300:118–30
Gioia IM, Shaya EJ, Le Fèvre O, Falco EE, Luppino G, Hammer F. 1998. *Ap. J.* 497:573–86
Gioia IM, Maccacaro T, Schild RE, Wolter A, Stocke JT, Morris SL, Henry JP. 1990. *Ap. J. Suppl.* 72:567–619
Gioia IM, Henry JP, Mullis CR, Ebeling H, Wolter A. 1999. *Astron. J.* 117:2608–16
Girardi M, Fadda D, Escalera E, Giuricin G, Mardirossian F, Mezzetti M. 1997. *Ap. J.* 490:56–62
Gorenstein MV, Falco EE, Shapiro II. 1988. *Ap. J.* 327:693–711
Griffiths RE, Casertano S, Im M, Ratnatunga KU. 1996. *MNRAS* 282:1159–64

Guiderdoni B, 1998. In *The Young Universe*, ed. S D'Odorico, A Fontana, E Giallongo, pp. 283–88. PASP Conf. Series. Vol. 146
Gunn J. E. 1967. *Ap. J.* 150:737–53
Hamana T, Hattori M, Ebeling H, Henry P, Futumase T, Shioya Y. 1997. *Ap. J.* 484:574–80
Hammer F, Rigaud F. 1989. *Astron. Astrophys.* 226:45–56
Hammer F, Teyssandier P, Shaya EJ, Gioia IM, Luppino GA. 1997. *Ap. J.* 491:477–82
Hattori M, Ibeke Y, Asaoka I, Takeshima T, Böhringer H, Mihara T, Neumann DM, Schindler S, Tsuru T, Tamura T. 1997. *Nature* 388:146–48
Hattori M, Watanabe K, Yamashita K. 1997. *Astron. Astrophys.* 319:764–80
Hoekstra H, Franx M, Kuijken K, Squires G. 1998. *Ap. J.* 504:636–60
Hudson MJ, Gwyn S, Dahle H, Kaiser N. 1998. *Ap. J.* 503:531–42
Im M, Griffiths RE, Ratnatunga KU. 1997. *Ap. J.* 475:457–61
Ivison RJ, Smail I, Le Borgne J-F, Blain AW, Kneib J-P, Bézecourt J, Kerr TH, Davies JK. 1998. *MNRAS* 298:583–93
Jain B, Seljak U. 1997. *Ap. J.* 484:560–73
Jain B, Seljak U, White S. 1998. In *Fundamental Parameters in Cosmology*, ed. J Tran Thanh Van, Y Giraud-Héraud, F Bouchet, T Damour, Y Millier. Les Arcs: Frontières
Kaiser N. 1992. *Ap. J.* 388:272–86
Kaiser N. 1995. *Ap. J. Lett.* 439:L1–3
Kaiser N. 1998. *Ap. J.* 498:26–42
Kaiser N, Squires G. 1993. *Ap. J.* 404:441–50
Kaiser N, Squires G, Broadhurst T. 1995. *Ap. J.* 449:460–75
Kaiser N, Wilson G, Luppino G, Kofman L, Gioia I, Metzger M, Dahle H. 1998. Preprint astro-ph/9809268
Kamionkowski M, Babul A, Cress CM, Réfrégier A. 1998. *MNRAS* 301:1064–72
Kassiola A, Kovner I, Fort B. 1992a. *Ap. J.* 400:41–57
Kassiola A, Kovner I, Blandford RD. 1992b. *Ap. J.* 396:10–19
Kneib J-P, Mellier Y, Fort B, Mathez G. 1993. *Astron. Astrophys.* 273:367–76
Kneib J-P, Mathez G, Fort B, Mellier Y, Soucail G, Longaretti P-Y. 1994. *Astron. Astrophys.* 286:701–17
Kneib J-P, Mellier Y, Pelló R, Miralda-Escudé J, Le Borgne J-F, Böhringer H, Picat J-P. 1995. *Astron. Astrophys.* 303:27–40
Kneib J-P, Ellis RS, Smail I, Couch W, Sharples RM. 1996. *Ap. J.* 471:643–56
Kneib J-P, Alloin D, Mellier Y, Guilloteau S, Barvainis R, Antonucci R. 1998. *Astron. Astrophys.* 329:827–39
Kochanek CS, Blandford RD, Lawrence CR, Narayan R. 1989. *MNRAS* 238:43–56
Kochanek CS. 1990. *MNRAS* 247:135–51
Kochanek CS. 1991. *Ap. J.* 373:354–68
Kochanek CS. 1995. *Ap. J.* 445:559–77
Kochanek CS. 1996. *Ap. J.* 466:638–59
Kovner I, Milgrom M. 1987. *Ap. J. Lett.* 321:L113–15
Krauss LM. 1998. Preprint astro-ph/9807376
Kristian J, Sachs RK. 1966. *Ap. J.* 143:379–86
Kristian J. 1967. *Ap. J.* 147:864–67
Kruse G, Schneider P. 1999. *MNRAS* 302:821–29
Lémonon L, Pierre M, Cesarsky C, Elbaz D, Pelló R, Soucail G, Vigroux L. 1998. *Astron. Astrophys. Lett.* 334:L21–25
Link R, Pierce M. 1998. *Ap. J.* 502:63–74
Lombardi M, Bertin G. 1998a. *Astron. Astrophys.* 330:791–800
Lombardi M, Bertin G. 1998b. *Astron. Astrophys.* 335:1–11
Lombardi M, Bertin G. 1999. *Astron. Astrophys.* 342:337–52
Luppino G, Kaiser N. 1997. *Ap. J.* 475:20–28
Lynds R, Petrosian V. 1986. *BAAS* 18:1014
Maddox SJ, Efstathiou G, Sutherland WJ, Loveday J. 1990. *MNRAS* 243:692–712
Markevitch M. 1997. *Ap. J. Lett.* 483:L17–20
Martínez-González E, Sanz JL, Cayón L. 1997. *Ap. J.* 484:1–6
Mellier Y. 1997. In *The Hubble Space Telescope and the High Redshift Universe*, ed. NR Tanvir, A Aragón-Salamanca, JV Wall. pp. 237–48. Cambridge: World Scientific
Mellier Y, Fort B, Soucail G, Mathez G, Cailloux M. 1991. *Ap. J.* 380:334–43

Mellier Y, Fort B, Kneib J-P. 1993. *Ap. J.* 407:33–45
Mellier Y, Dantel-Fort M, Fort B, Bonnet H. 1994. *Astron. Astrophys. Lett.* 289:L15–18
Mellier Y, Van Waerbeke L, Bernardeau F, Fort B. 1997. In *Neutrinos, Dark Matter and the Universe*, ed. T Stolarcyk, J Tran Thanh Van, F Vannucci, pp. 191–204. Paris: Frontières
Metcalf B, Silk J. 1997. *Ap. J.* 489:1–6
Metcalf B, Silk J. 1998. *Ap. J. Lett.* 492:L1–4
Miralda-Escudé J. 1991. *Ap. J.* 380:1–8
Miralda-Escudé J, Babul A. 1995. *Ap. J.* 449:18–27
Moessner R, Jain B. 1998. *MNRAS Lett.* 294:L18–24
Moessner R, Jain B, Villumsen J. 1998. *MNRAS* 294:291–98
Mould J, Blandford R, Villumsen J, Brainerd T, Smail I, Small T, Kells W. 1994. *MNRAS* 271:31–38
Nakamura TT 1997. *Publ. Astron. Soc. Japan* 49:151–57
Nakanishi K, Ohta K, Takeuchi TT, Akiyama M, Yamada T, Shioya Y. 1997. *Publ. Astron. Soc. Japan* 49:535–38
Navarro JF, Frenk CS, White SDM. 1997. *Ap. J.* 490:493–508
Natarajan P, Kneib J-P. 1997. *MNRAS* 287:833–47
Natarajan P, Kneib J-P, Smail I, Ellis RS. 1998. *Ap. J.* 499:600–7
Ota N, Mitsuda K, Fukazawa Y. 1998. *Ap. J.* 495:170–78
Paczynski B, Gorski K. 1981. *Ap. J. Lett.* 248:L101–4
Peacock JA, Dodds S. 1996. *MNRAS Lett.* 280:L19–26
Pelló R, Sanahuja B, Le Borgne J-F, Soucail G, Mellier Y. 1991. *Ap. J.* 366:405–11
Pelló R, Miralles J-M, Le Borgne J-F, Picat J-P, Soucail G, Bruzual G. 1996. *Astron. Astrophys.* 314:73–86
Pierre M, Le Borgne J-F, Soucail G, Kneib J-P. 1996. *Astron. Astrophys.* 311:413–24
Puget J-L, Abergel A, Boulanger F, Bernard J-P, Burton WB, Désert F-X, Hartmann D. 1996. *Astron. Astrophys.* 308:L5–8
Reblinksy K, Bartelmann M. 1999. *Astron. Astrophys.* 345:1–6
Réfrégier A, Brown ST. 1998. Preprint astro-ph/9803279
Refsdal S. 1964. *MNRAS* 128:307–10
Refsdal S, Surdej J. 1994. *Rep. Prog. Phys.* 56:117–85
Rodrigues-Williams LL, Hogan CJ. 1994. *Astron. J.* 107:451–60
Rosati P. 1999. In *Wide Field Surveys in Cosmology*, ed. S Colombi, Y Mellier, B Raban. pp. 219–29. Paris: Frontières
Sachs RK. 1961. *Proc. R. Soc. London* A264:309
Sahu KC, Shaw RA, Kaiser ME, Baum SA, Fergusson HC, Hayes JJE, Gull TR, Hill RJ, Hutchings JB, Kimble RA, Plait P, Woodgate BE, et al. 1998. *Ap. J. Lett.* 492:L125–29
Sanz JL, Martínez-González E, Benítez N. 1997. *MNRAS* 291:418–24
Saraniti DW, Petrosian V, Lynds R. 1996. *Ap. J.* 458:57–66
Schindler S, Hattori M, Neumann DM, Böhringer H. 1997. *Astron. Astrophys.* 317:646–55
Schneider P. 1992. *Astron. Astrophys.* 254:14–24
Schneider P. 1995. *Astron. Astrophys.* 302:639–48
Schneider P. 1998. *Ap. J.* 498:43–47
Schneider P, Weiss A. 1988. *Ap. J.* 327:526–43
Schneider P, Ehlers J, Falco EE. 1992. In *Gravitational Lenses*. New York: Springer
Schneider P, Rix HW. 1997. *Ap. J.* 474:25–36
Schneider P, Seitz C. 1995. *Astron. Astrophys.* 294:411–31
Schneider P, Kneib J-P. 1999. In *The Next Generation Space Telescope: Science Drivers and Technological Challenges*, ed. P Benvenuti et al. ESA SP-429
Schneider P, Van Waerbeke L, Mellier Y, Jain B, Seitz S, Fort B. 1998a. *Astron. Astrophys.* 333:767–78
Schneider P, Van Waerbeke L, Jain B, Kruse G. 1998b. *MNRAS* 296:873–92

Schramm T, Kayser R. 1995. *Astron. Astrophys.* 299:1–10
Seitz C, Kneib J-P, Schneider P, Seitz S. 1996. *Astron. Astrophys.* 314:707–20
Seitz C, Schneider P. 1995a. *Astron. Astrophys.* 297:287–99
Seitz C, Schneider P. 1997. *Astron. Astrophys.* 318:687–99
Seitz S, Collodel L, Pirzkal N, Erben T, Freudling W, Schneider P, Fosbury R, White SDM. 1999. In *Wide Field Surveys in Cosmology*, ed. S Colombi, Y Mellier, B Raban, pp. 203–8. Paris: Frontières
Seitz S, Saglia RP, Bender R, Hopp U, Belloni P, Ziegler B. 1998b. *MNRAS* 298:945–65
Seitz S, Schneider P. 1995b. *Astron. Astrophys.* 302:9–20
Seitz S, Schneider P. 1996. *Astron. Astrophys.* 305:383–401
Seitz S, Schneider P, Bartelmann M. 1998a. *Astron. Astrophys.* 337:325–37
Seljak U. 1996. *Ap. J.* 463:1–7
Seljak U. 1998. *Ap. J.* 506:64–79
Seljak U. 1997. *Ap. J.* 482:6–16
Smail I. 1993. *Gravitational Lensing by Rich Clusters of Galaxies*. PhD Thesis, University of Durham
Smail I, Ellis RS, Aragón-Salamanca A, Soucail G, Mellier Y, Giraud E. 1993. *MNRAS* 263:628–40
Smail I, Ellis RS, Fitchett M. 1994. *MNRAS* 270:245–70
Smail I, Ellis RS, Fitchett M, Edge AC. 1995a. *MNRAS* 273:277–94
Smail I, Couch W, Ellis RS, Sharples RM. 1995b. *Ap. J.* 440:501–9
Smail I, Dickinson M. 1995. *MNRAS* 455:L99–102
Smail I, Hogg DW, Yan L, Cohen JG. 1995c. *Ap. J. Lett.* 449:L105–8
Smail I, Ellis RS, Dressler A, Couch WJ, Oemler A, Sharples R, Butcher H. 1997a. *Ap. J.* 479:70–81
Smail I, Ivison RJ, Blain AW. 1997b. *Ap. J. Lett.* 490:L5–8
Smail I, Ivison RJ, Blain AW, Kneib J-P. 1999. *MNRAS* 302:632–48
Smooth GF, Bennett CL, Kogut A, Wright EL, Aymon J, Boggess NW, Cheng ES, De Amici G, Gulkis S, Hauser MG, Hinshaw G, Jackson DD, Janssen M, Kaita E, Kelsall T, Keegstra P, Lineweaver G, Loewenstein K, Lubin P, Mather J, Meyer SS, Moseley SH, Murdock T, Rokke L, Silverberg RF, Tenorio L, Weiss R, Wilkinson DT, et al. 1992. *Ap. J. Lett.* 396:L1–5
Soifer BT, Neugebauer G, Franx M, Matthews K, Illingworth GD. 1998. *Ap. J.* 501:L171–74
Soucail G, Fort B, Mellier Y, Picat J-P. 1987. *Astron. Astrophys. Lett.* 172:L14–17
Soucail G, Mellier Y, Fort B, Mathez G, Cailloux M. 1998. *Astron. Astrophys. Lett.* 191:L19–22
Squires G, Kaiser N, Babul A, Fahlman G, Woods D, Neumann DM, Böhringer H. 1996a. *Ap. J.* 461:572–86
Squires G, Kaiser N, Fahlman G, Babul A, Woods D. 1996b. *Ap. J.* 469:73–77
Squires G, Kaiser N. 1996. *Ap. J.* 473:65–80
Squires G, Neumann DM, Kaiser N, Arnaud M, Babul A, Böhringer H, Fahlman G, Woods D. 1997. *Ap. J.* 482:648–58
Stebbins A. 1996. Preprint astro-ph/9609149
Stebbins A. 1999. In *Wide Field Surveys in Cosmology*, ed. S Colombi, Y Mellier, B Raban, pp. 197–201. Paris: Frontières
Steidel C, Adelberger K, Giavalisco M, Dickinson M, Pettini M, Kellogg M. 1998. In *The Young Universe*, ed. S D'Odorico, A Fontana, E Giallongo, pp. 428–35. PASP Conf. Series. Vol. 146
Stompor R, Efstathiou G. 1999. *MNRAS* 302:735–47
Szapudi I, Colombi S. 1996. *Ap. J.* 470:131–48
Taylor AN, Dye S, Broadhurst TJ, Benítez N, Van Kampen E. 1998. *Ap. J.* 501:539
Tomita K, Watanabe K. 1990. *Prog. Theo. Phys.* 83:467–90
Trager SC, Faber SM, Dressler A, Oemler A. 1997. *Ap. J.* 485:92–99
Tyson JA. 1985. *Nature* 316:799–800

Tyson JA, Valdes F, Jarvis JF, Mills AP. 1984. *Ap. J. Lett.* 281:L59–62
Tyson JA. 1988. *Astron. J.* 96:1–23
Tyson JA, Valdes F, Wenk RA. 1990. *Ap. J. Lett.* 349:L1–4
Tyson JA, Fischer P. 1995. *Ap. J. Lett.* 446:L55–58
Tyson JA, Kochanski GP, Dell'Antonio IP. 1998. *Ap. J. Lett.* 498:L107–10
Valdes F, Tyson JA, Jarvis JF. 1983. *Ap. J.* 271:431–41
Van Kampen E. 1998. *MNRAS* 301:389–404
Van Waerbeke L. 1998a. *Astron. Astrophys.* 334:1–10
Van Waerbeke L. 1998b. In *Wide Field Surveys in Cosmology.* pp. 189–93. Paris: Frontières
Van Waerbeke L. 1999. *MNRAS.* In press
Van Waerbeke L, Mellier Y. 1997. In *Proceedings of the XXXIst Rencontres de Moriond*. Les Arcs: Frontières
Van Waerbeke L, Mellier Y, Schneider P, Fort B, Mathez G. 1997. *Astron. Astrophys.* 317:303–17
Van Waerbeke L, Bernardeau F, Mellier Y. 1999. *Astron. Astrophys.* 342:15–33
Villumsen JV. 1996. *MNRAS* 281:369–83
Wambsganss J, Cen R, Ostriker JP. 1998. *Ap. J.* 494:29–46
Wallington S, Kochanek CS, Koo DC. 1995. *Ap. J.* 441:58–69
Walsh D, Carswell RF, Weymann RJ. 1979. *Nature* 279:381
Webster R. 1985. *MNRAS* 213:871–88
White M. 1998. Preprint astro-ph/9802295
White M, Scott D, Silk J. 1994. *Annu. Rev. Astron. Astrophys.* 32:319–70
Williams LLR, Irwin M. 1998. *MNRAS* 298:378–386
Wilson G, Cole S, Frenk CS. 1996a. *MNRAS* 280:199–218
Wilson G, Cole S, Frenk CS. 1996b. *MNRAS* 282:501–10
Wu X-P, Mao S. 1996. *Ap. J.* 463:404–8
Wu X-P, Fang L-Z. 1996. *Ap. J.* 461:L5–8
Wu X-P, Fang L-Z. 1997. *Ap. J.* 483:62–67
Zaldarriaga M, Seljak U. 1998. Preprint astro-ph/9803150
Zel'dovich YB. 1964. *Sov. Astron.* 8:13–16
Zhu Z-H, Wu X-P. 1997. *Astron. Astrophys.* 324:483
Zwicky F. 1933. *Helv. Phys. Acta* 6:10
Zwicky F. 1937. *Phys. Rev.* 51:290